Mathematical Biosciences and Engineering

MBE, 20 (10): 17747–17782.
DOI: 10.3934/mbe.2023789
Received: 01 June 2023
Revised: 26 August 2023
Accepted: 26 August 2023
Published: 18 September 2023

http://www.aimspress.com/journal/MBE

Research article

Comparison, validation and improvement of empirical soil moisture models for conditions in Colombia

Alejandro Rincón[1,2], Fredy E. Hoyos[3] and John E. Candelo-Becerra[3,*]

[1] Grupo de Investigación en Desarrollos Tecnológicos y Ambientales (GIDTA), Facultad de Ingeniería y Arquitectura, Universidad Católica de Manizales, Carrera 23 N. 60–63, Manizales 170002, Colombia.
[2] Grupo de Investigación en Microbiología y Biotecnología Agroindustrial (GIMIBAG), Instituto de Investigación en Microbiología y Biotecnología Agroindustrial, Universidad Católica de Manizales, Carrera 23 N. 60–63, Manizales 170002, Colombia.
[3] Departamento de Energía Eléctrica y Automática, Facultad de Minas, Universidad Nacional de Colombia, Sede Medellín, Carrera 80 No. 65–223, Campus Robledo, Medellín 050041, Colombia.

* **Correspondence:** Email: jecandelob@unal.edu.co; Tel: +57(604)4255000.

Abstract: Modeling soil moisture as a function of meteorological data is necessary for agricultural applications, including irrigation scheduling. In this study, empirical water balance models and empirical compartment models are assessed for estimating soil moisture, for three locations in Colombia. The daily precipitation and average, maximum and minimum air temperatures are the input variables. In the water balance type models, the evapotranspiration term is based on the Hargreaves model, whereas the runoff and percolation terms are functions of precipitation and soil moisture. The models are calibrated using field data from each location. The main contributions compared to closely related studies are: i) the proposal of three models, formulated by combining an empirical water balance model with modifications in the precipitation, runoff, percolation and evapotranspiration terms, using functions recently proposed in the current literature and incorporating new modifications to these terms; ii) the assessment of the effect of model parameters on the fitting quality and determination of the parameters with higher effects; iii) the comparison of the proposed empirical models with recent empirical models from the literature in terms of the combination of fitting accuracy and number of parameters through the Akaike Information Criterion (AIC), and also the Nash-Sutcliffe (NS) coefficient and the root mean square error. The best models described soil moisture with an NS efficiency higher than 0.8. No single model achieved the highest performance for the three locations.

The VJRAM, HDG0 and HDG0 models achieved the lowest AIC values for Naranjal, Calarcá and Balboa weather stations, respectively, with NS values of 0.895, 0.653 and 0.983, respectively. The proposed modifications improved soil moisture simulation at the three locations.

Keywords: soil moisture model; evapotranspiration; hydrology; effective rainfall; Hargreaves model; coffee crop; simulation model

1. Introduction

Soil moisture (SM) is an important variable in water and energy fluxes occurring at the interface between land surface and atmosphere [1–4]. SM influences the surface energy, and it is a key feature in the partitioning of the net radiation into sensible heat and latent heat [1,5], the partitioning of rainfall into runoff, percolation and evapotranspiration [1,6], the plant photosynthesis and respiration [7–10], plant transpiration [10,11] and plant growth and physiological state [12–14]. SM is widely used in several disciplines, including: earth system dynamics, water resource management, agriculture, forestry and soil science [15,16]. In agriculture, SM is used for studies on crop production and for determining irrigation requirements [7,17–19]. In the event of soil moisture stress, productivity is seriously affected, and the plant has to consume more energy to take water from the soil [7,20].

SM models allow for the reduction of regular measurements of soil moisture, which is expensive and time consuming. In addition, soil moisture is only measured in special cases [21,22]. Physically-based models are based on the water transport in the soil-plant-root system, and they use the mass balance of soil water in the crop root zone, with terms for effective precipitation (P_{ef}), evapotranspiration (E), runoff (R) and percolation (G). These terms aim at providing realistic estimates of these physical processes. Extensive field data (including soil characteristics) are required for estimating model parameters, so its applicability is limited [23]. The empirical models emerged later, using the balance of the water mass with nonlinear functions related to P_{ef}, E, R and G, aimed at obtaining an accurate estimation of the SM; however, a realistic estimation of physical processes is not intended [22,24]. They use available meteorological data, requiring few or no soil characteristics, their tuning is simple and they can achieve high performance with high r^2 values [22,25].

In [22], an empirical model is proposed for estimating soil moisture in a Himalayan watershed. It comprises the classical soil water balance. However, simplified empirical relations are used for infiltration, evapotranspiration and percolation: i) the infiltration term is a function of only rainfall, and it comprises a power law relation; ii) the percolation term is a function of only soil moisture and infiltration; iii) the evapotranspiration term is a function of only air temperature, soil surface temperature and wind speed. Therefore, the input variables of the model are rainfall, wind speed, air temperature and soil surface temperature. The model is calibrated with measurements from three sites at the lesser Himalaya for three soil depths. The performance of the model decreases as the depth of the soil increases.

In [26], a set of simplified models is proposed for estimating the soil moisture, and it is calibrated to data from Taranaki, New Zealand. Each model comprises a first-order differential equation, with empirical terms depending on rainfall, soil temperature, soil moisture and day length. A loss term is included, which depends on soil moisture level, soil, the temperature of the soil and the length of the day. The models were calibrated with data from ten locations in the Taranaki region in New Zealand.

Despite their simplicity, the models can be used for sites with different soil characteristics and soil moisture dynamics. The negative soil moisture term proved significant in sites with soil moisture levels above field capacity, whereas the term involving temperature and daylight proved significant in sites with soil moisture levels below field capacity.

In [21], an adaptive neurofuzzy inference system (ANFIS) is used for estimating soil moisture at the Istanbul Bolge station in Turkey, considering the classical ANFIS model and its coupling with three bioinspired metaheuristic optimization methods: ANFIS coupled with the whale optimization algorithm (ANFIS-WOA), ANFIS coupled with the krill herd algorithm (ANFIS-KHA) and ANFIS coupled with the firefly algorithm (ANFIS-FA). The input variables are the daily air temperature, relative humidity, wind speed, sunshine hours and soil temperature. The models were calibrated with data from Turkey, 2008–2009. The SM estimation with hybrid models (ANFIS-WOA, ANFIS-KHA and ANIFS-FA) achieved a significantly lower estimation error compared to the classical ANFIS model. Furthermore, the performance of the model for different soil moisture intervals was: 15–25% (first interval), 25–35% (middle interval) and ≥35% (last interval). Hybrid models had better performance for the last interval and worst performance for the middle interval. The ANFIS-WOA model had the best performance, considering each of the three SM intervals and considering the entire SM range.

In [7], a simple model is used for estimating soil moisture and calculating irrigation requirements, in the Sikkim state of India. The model comprises a discretized soil water balance model, with an effective rainfall term, an evapotranspiration term and a constant term; a multiplicative coefficient is incorporated into the rainfall and evapotranspiration terms. The effective rainfall term is a nonlinear piecewise function of rainfall. The input variables of the model are rainfall, daily maximum and minimum temperatures, relative humidity, wind speed, precipitation and sunshine hours. The model was calibrated with data from three meteorological stations located in different parts of the Sikkim state, from the 2015–2016 period, and then validated using data from the 2016–2017 period. The determination coefficients were 0.76, 0.66 and 0.63 for the stations. Additionally, irrigation requirements for cabbage, mustard green leaves, potato, broccoli and cauliflower were calculated for the three locations.

In this work, several empirical models are used for estimating soil moisture in three locations of Colombia, considering limited weather data. The input variables are the daily maximum, minimum and average air temperatures, and precipitation. The first model (HDG0) is based on water balance and the Hargreaves model is used for the evapotranspiration term, while the runoff and percolation components are functions of precipitation and soil moisture. The second model (VJRAM) is based on water balance, where the evapotranspiration term uses the Hargreaves model and the runoff and percolation terms are functions of precipitation. The third model (K) is a simple compartment model, involving terms related to gain from rainfall and soil moisture loss, considering daylight and temperature effects. In addition, two models are proposed, formulated by combining the first model with modifications in the precipitation, runoff, percolation and evapotranspiration terms, using functions recently proposed in the current literature. Each model is calibrated using data from each location, and the fitting quality of the models is compared for each location. Compared to previous related studies on SM modeling using empirical models, the main contributions of this paper are the following:

i) Based on the model in [27], a new model is proposed with terms from the recent literature.

ii) The effect of model parameters on the fitting quality is assessed and the parameters with higher effect are determined.
iii) The proposed models and the empirical models found in the recent literature are compared in terms of the combination of fitting accuracy and number of parameters, through the Akaike Information Criterion (AIC).

2. Soil moisture models

Precipitation turns into runoff, percolation and evapotranspiration, so that the soil moisture dynamics depends on these components [25,28,29]. Furthermore, a part of precipitated water evaporates into the atmosphere before it reaches the top soil layer [1], and the other part is retained by plant cover [30–32]. The part of precipitation that can be used by the plant root is known as effective precipitation [1].

Soil moisture (SM) is influenced by topography, soil properties (soil texture, drainage capability and soil density), vegetation and meteorological conditions (e.g. precipitation, temperature, wind speed) [1,33–35]. SM exhibits spatial variation due to its dependence on local soil characteristics [25]. Soil density influences root growth, movement of air and water through the soil and infiltration rates [7]. Additionally, the vegetation type and density affect the soil water content and soil hydrological processes [12]. Precipitation and temperature are considered as the meteorological variables with major effect on SM [22,33], and there is a strong correlation of soil moisture with temperature and precipitation [36]. SM decreases with air temperature, wind speed and solar radiation through evapotranspiration [22].

The water balance model considers the partition of precipitation into effective precipitation (infiltration), runoff, percolation and evapotranspiration, so that the soil moisture dynamics depend on these terms [28]. Evapotranspiration is commonly estimated with the Penman-Monteith (PM) model, which comprises air temperature, air relative humidity, wind speed and solar radiation as input variables. However, evapotranspiration can also be estimated with the Hargreaves (HG) model, mainly in the case where measurements of air relative humidity, wind speed and solar radiation are missing [24,37–39]. It can provide a satisfactory representation of evapotranspiration, achieving high values of the determination coefficient [39], and it has proven effective in estimating rainfall with effectiveness indexes similar to those of the PM model (see [24]).

2.1. Water balance and evapotranspiration models

The water balance is [3,24,40]:

$$D\frac{dW}{dt} = P_{ef,k} - E_k - R_k - G_k.$$

The term D is the product of soil depth and porosity, W is the soil moisture, P_{ef} is the effective rainfall, E is the evapotranspiration, R is the streamflow divergence (runoff) and G is the loss of groundwater through deep percolation. The D coefficient can be combined with the coefficients of $P_{ef,k}$, E_k, R_k and G_k, so that:

$$\frac{dW}{dt} = P_{ef} - E - R - G. \tag{1}$$

Evapotranspiration can be expressed as in Eq (2) [24,25]:

$$E = f(W)ET_0, \tag{2}$$

where $f(W)$ is a function of W and ET_0 is the reference evapotranspiration [mm/day]. ET_0 is usually calculated through the Penman-Monteith equation derived by the United Nations Food and Agriculture Organization (FAO), but the Hargreaves equation can be used for the case that solar radiation, air relative humidity and wind speed are not available [24,37,38,41,42]:

$$ET_0 = 0.0018\big(T_{avg} + 17.8\big)(T_{max} - T_{min})^{0.5}R_a, \tag{3}$$

where T_{avg} (°C) is the daily averaged air temperature (°C); T_{max} and T_{min} are the daily maximum and daily minimum air temperature (°C); R_a is the extraterrestrial radiation. The R_a equations are provided in [42]. The Hargreaves model in Eq (3) can be combined with a constant term and a multiplicative coefficient (see [42]):

$$ET_0 = max\big\{0,\ k_{E1}0.0018\big(T_{avg} + 17.8\big)(T_{max} - T_{min})^{0.5}R_a - k_{E2}\big\}, \tag{4}$$

where k_{E1} and k_{E2} are constant coefficients. All the coefficients, not only k_{E1} and k_{E2}, can be fitted to experimental data (see [39,41]). Some examples of the term $f(W)$ in Eq (2) are [24,27]:

$$f(W) = W;\ f(W) = \frac{W}{W_{max}};$$

$$f(W) = \begin{cases} k_e W + \frac{k_{cb}}{k_p} W \ \ for\ \ W < k_p \\ k_e W + k_{cb} \ \ for\ \ W \geq k_p \end{cases},$$

where W_{max}, k_e, k_{cb} and k_p are positive constants.

2.2. VJRAM model

Effective rainfall, runoff and percolation for unshaded coffee are represented as [43]:

$$P_{ef} = 0.92P;\ R = \begin{cases} 0.027P\ for\ P \geq 20mm \\ 0\ otherwise \end{cases},$$

$$G = \begin{cases} 9.94Ln(P) - 11.84\ for\ P > 0.972 \\ 0\ otherwise \end{cases}.$$

However, the measurements given in [43] and [32] indicate that P_{ef}, R and G exhibit a dead zone for low rainfall values, so that the above relations can be improved as:

$$R = \begin{cases} k_R(P - P_R) \ \ for\ P \geq P_R \\ 0\ otherwise \end{cases};\ G = \begin{cases} k_{G1}Ln(P) - k_{G1}Ln(P_G) \ \ for\ P > P_G \\ 0\ otherwise \end{cases};$$

where k_R P_R k_{G1} and P_G are constant. In [44], the evapotranspiration is expressed as $E = ET_0(W/k_{ws})$, where k_{ws} is a constant, and several equations are suggested for ET_0. Using the above expressions, the VJRAM model is given by Eq (1) with P_{ef}, E, R, and G terms defined as:

$$\begin{bmatrix} P_{ef} = k_p P \\ E = ET_0 W \\ R = max\{0, k_{R1} P - k_{R2}\} \\ G = max\{0, k_{G1} Ln(P) - k_{G2}\} \end{bmatrix}, \tag{5}$$

where ET_0 is given by Eq (4). The parameters to be estimated are: k_p, k_{R1}, k_{R2}, k_{G1}, k_{G2}, k_{E1} and k_{E2}.

2.3. K models

The K8 model is the model (8) in [26]:

$$\frac{dW}{dt} = -\alpha_1 W - \alpha_{1b} W \left(\frac{\alpha_{1c} + \alpha_{1d} T_{air}}{20}\right)\left(\frac{D_L}{12}\right) + \alpha_2 P + \alpha_{2b} P \left(\frac{30}{W}\right). \tag{6}$$

The term W is the soil moisture, P is the precipitation (mm), T_{air} is the air temperature in degrees Celsius, D_L is the day length (hours), whereas α_1, α_{1b}, α_{1c}, α_{1d}, α_2 and α_{2b} are constant parameters to be estimated. In order to overcome the lack of soil temperature data, the relationship $T_s = \alpha_{1c} + \alpha_{1d} T_{air}$ where T_s is the soil temperature, taken from [45]. The $-\alpha_{1b} W (T_s/20)(D_L/12)$ term represents the soil moisture loss due to transpiration and evaporation, whereas the $-\alpha_1 W$ term represents runoff and percolation. The day length (D_L) equation is given in [46]. The model requires daily precipitation and daily average air temperature as input data. The parameters to be estimated are: α_1, α_{1b}, α_{1c}, α_{1d}, α_2, and α_{2b}.

The K7 model is a combination of model (7) from [26] with the $\alpha_2 P$ term:

$$\frac{dW}{dt} = -\alpha_1 W - \alpha_{1b} W \left(\frac{\alpha_{1c} + \alpha_{1d} T_{air}}{20}\right) + \alpha_2 P + \alpha_{2b} P \left(\frac{30}{W}\right). \tag{7}$$

The parameters to be estimated are: α_1, α_{1b}, α_{1c}, α_{1d}, α_2 and α_{2b}.

2.4. HDG0 model

The HDG0 model is given by Eq (1) with P_{ef}, E, R and G terms [27]:

$$\begin{bmatrix} P_{ef} = k_p \mathrm{P}; \\ E = ET_0 \frac{W}{W_{max}}; \\ R + G = P \left(\frac{W}{W_{max}}\right)^m + \alpha W, \ \ m > 1 \end{bmatrix}, \tag{8}$$

where W_{max} is the capacity of soil to hold water; m, W_{max}, α, and μ are constants. Substituting the P_{ef}, E and $R + G$ expressions into Eq (1), gives:

$$\frac{dW}{dt} = k_p P - ET_0 \frac{W}{W_{max}} - P \left(\frac{W}{W_{max}}\right)^m - \alpha W$$
$$m > 1.$$

In [27], the Thornthwaite formulas are used for ET_0, whereas we use Eq (4). The parameters to be estimated are: k_p, W_{max}, m, α, k_{E1} and k_{E2}.

2.5. HDG4 model

The HDG4 model is obtained by combining the HDG0 model with modification of the terms given in Table 1.

Table 1. Models for runoff, groundwater recharge and effective rainfall.

Model	Reference
$\boldsymbol{R+G=G}$; $\boldsymbol{G=aW^b}$, where $\boldsymbol{a>0}$, and $\boldsymbol{b>1}$ are constant.	[24]
$\boldsymbol{P_{ef}=\alpha P^{\beta}}$	
$\boldsymbol{R+G=G}$; $\boldsymbol{G=[exp(k_1P^n)][exp(k_2W)]}$ where $\boldsymbol{\alpha}$, $\boldsymbol{\beta}$ are constant, in the range $[\boldsymbol{0\ 1}]$; $\boldsymbol{k_1>0}$, $\boldsymbol{k_2>0}$, and $\boldsymbol{n<1}$ are constant.	[22]
$\boldsymbol{R=PW^c}$ $\boldsymbol{G=aW^b}$ where $\boldsymbol{a}$, $\boldsymbol{b}$, and $\boldsymbol{c}$ are constant.	[3]
$\boldsymbol{R+G=P\left(\frac{W}{W_{max}}\right)^m+\alpha W}$ where $\boldsymbol{W_{max}}$, $\boldsymbol{m}$, $\boldsymbol{\alpha}$, are constant.	[27]
$\boldsymbol{G=C_E{}^{-b_EF}C_E{}^{b_EW}}$ where $\boldsymbol{C_E}$, $\boldsymbol{b_E}$, and $\boldsymbol{F}$ are constant (Potential recharge empirical model).	[47]
$\boldsymbol{R=\begin{cases}\frac{(P-c_1)^2}{P+c_2} & for\ P>c_1\\ 0 & for\ P\le c_1\end{cases}}$ where $\boldsymbol{c_1}$ and $\boldsymbol{c_2}$, are constant (Curve number method)	[25,48]
$\boldsymbol{R+G=\alpha_1 W}$ Where $\boldsymbol{\alpha_1}$ is constant.	[26]
$\boldsymbol{P_{ef}=k_pP}$; $\boldsymbol{R=\begin{cases}k_RP & for\ P\ge P_R\\ 0 & otherwise\end{cases}}$; $\boldsymbol{G=\begin{cases}k_{G1}Ln(P)-k_{G2} & for\ P>P_G\\ 0 & otherwise\end{cases}}$	[43]

where $\boldsymbol{k_p}$, $\boldsymbol{k_R}$, $\boldsymbol{k_{G1}}$, $\boldsymbol{k_{G2}}$, $\boldsymbol{P_R}$, and $\boldsymbol{P_G}$ are constant.

Runoff (R) and percolation (G) terms vanish for precipitation lower than some threshold [44,48], whereas the effective precipitation data given in [32] indicate that P_{ef} vanishes for rainfall below some threshold. Then, we consider the dead zone function of precipitation:

$$\bar{P} = \begin{cases} P - P_{linf} & for\ P > P_{linf} \\ 0 & otherwise \end{cases},$$

where P_{linf} is a positive constant. The soil moisture time series for Balboa (Figure A3) indicates that for SM lower than a threshold, the rate of decrease in SM is overly slow. To account for this, we consider a dead zone function of SM:

$$\bar{W} = \begin{cases} W - W_{linf} & for\ W > W_{linf} \\ 0 & otherwise \end{cases},$$

where W_{linf} is a positive constant. The modifications presented in Table 2 are proposed to give a wider capability of describing the nonlinear nature of P_{ef} and $R + G$, based on the terms stated in Table 1.

Table 2. Modifications proposed for P_{ef}, $R + G$.

Model term	Proposed modification
$\boldsymbol{P_{ef} = \alpha P^{\beta}}$	$P_{ef} = k_p \bar{P}^{m_{p2}}$
Where $\boldsymbol{\alpha}$ and $\boldsymbol{\beta}$ are constant in the range $[\mathbf{0}\ \ \mathbf{1}]$ [22]	Where k_p and m_{p2} are constant.
$\boldsymbol{R + G = aW^b}$ Where $\boldsymbol{a > 0}$, $\boldsymbol{b > 1}$ are constant [24]	$R + G = \bar{P}^{m_{p1}} \left(\alpha_3 \bar{W} + \left(\frac{\bar{W}}{W_{max}} \right)^{m_{w1}} \right) + \alpha_0 + \alpha_1 \bar{W} + \alpha_2 \bar{W}^{m_{w2}}$ Where m_{p1}, α_3, W_{max}, m_{w1}, α_0, α_1, α_2, and m_{w2} are constant.
$\boldsymbol{R + G = P\left(\frac{W}{W_{max}}\right)^m + \alpha W}$ Where $\boldsymbol{W_{max}}$, $\boldsymbol{m}$, and $\boldsymbol{\alpha}$, are constant [27]	
$\boldsymbol{R + G = PW^c + aW^b}$ Where $\boldsymbol{a}$, $\boldsymbol{b}$, and $\boldsymbol{c}$ are constant [3]	

In the evapotranspiration term, different values of the proportional coefficients are used for $P \leq P_{linf}$ and $P > P_{linf}$, where P_{linf} is a positive constant:

$$ET_T = \begin{cases} k_{E11} 0.0018 \left(T_{avg} + 17.8\right) \left(T_{max} - T_{min}\right)^{0.5} R_a - k_{E21} & for\ P > P_{linf} \\ k_{E12} 0.0018 \left(T_{avg} + 17.8\right) \left(T_{max} - T_{min}\right)^{0.5} R_a - k_{E22} & otherwise \end{cases}.$$

In summary, the HDG4 model is given by Eq (1) with P_{ef}, E, R and G terms:

$$\begin{bmatrix} P_{ef} = k_p \bar{P}^{m_{p2}} \\ E = ET_0 \frac{W}{W_{max}}, ET_0 = max\{0,\ ET_T\} \\ ET_T = \begin{cases} k_{E11} 0.0018\big(T_{avg} + 17.8\big)(T_{max} - T_{min})^{0.5} R_a \\ -k_{E21} \ \ for\ P > P_{linf} \\ k_{E12} 0.0018\big(T_{avg} + 17.8\big)(T_{max} - T_{min})^{0.5} R_a \\ -k_{E22} \ \ otherwise \end{cases} \\ R + G = \bar{P}^{m_{p1}} \left(\alpha_3 \overline{W} + \left(\frac{\overline{W}}{W_{max}}\right)^{m_{w1}}\right) + \alpha_0 + \alpha_1 \overline{W} + \alpha_2 \overline{W}^{m_{w2}} \end{bmatrix}, \tag{9}$$

where,

$$\bar{P} = \begin{cases} P - P_{linf} \ \ for \ \ P > P_{linf} \\ 0 \ \ otherwise \end{cases},$$

$$\overline{W} = \begin{cases} W - W_{linf} \ \ for\ W > W_{linf} \\ 0 \ \ otherwise \end{cases}.$$

The parameters to be estimated are: k_p, W_{max}, m_{w1}, α_1, k_{E11}, k_{E21}, α_0, α_3, α_2, m_{w2}, m_{p1}, m_{p2}, k_{E12} and k_{E22}.

2.6. HDG1 model

The HDG1 model is a simplification of the HDG4 model, comprising the following modifications of terms in Eq (9):

i) the evapotranspiration function Eq (4) is used instead of the piecewise function ET_T;
ii) only two additive terms are used for $R + G$;
iii) a Monod type function with dead zone is used for P_{ef}, wherein the Monod function is used to represent the non-linear increase of P_{ef} with P.

Then, the HDG1 model is given by Eq (1) with P_{ef}, E, R and G terms:

$$\begin{bmatrix} P_{ef} = \begin{cases} k_{p1} \frac{P}{k_{p2} + P} - k_{p1} \frac{P_{linf}}{k_{p2} + P_{linf}} \ for\ P > P_{linf} \\ 0 \ otherwise \end{cases} \\ E = ET_0 \frac{\overline{W}}{W_{max}}, ET_0 = max\big\{0,\ k_{E1} 0.0018\big(T_{avg} + 17.8\big)(T_{max} - T_{min})^{0.5} R_a - k_{E2}\big\} \\ R + G = P\left(\frac{\overline{W}}{W_{max}}\right)^m + \alpha \overline{W}^n \\ \overline{W} = \begin{cases} W - W_{linf} \ if\ W \geq W_{linf} \\ 0 \ 0therwise \end{cases} \end{bmatrix}. \tag{10}$$

The term W_{linf} is a positive constant that can be defined from data, or it can be set as zero if it is uncertain. The parameters to be estimated are: k_{p1}, k_{p2}, P_p, W_{max}, m, α, n, k_{E1} and k_{E2}. The resulting mass balance model is:

$$\frac{dW}{dt} = P_{ef} - ET_0 \frac{\overline{W}}{W_{max}} - P\left(\frac{\overline{W}}{W_{max}}\right)^m - \alpha \overline{W}^n.$$

2.7. HDG3 model

The HDG3 model is a simplification of the HDG4 model, obtained from the HDG4 model with a sole value of the proportional coefficients in the evapotranspiration term. Then, the HDG3 model is given by Eq (1) with P_{ef}, E and $R+G$ terms:

$$\begin{bmatrix} P_{ef} = k_p P; \\ E = ET_0 \frac{W}{W_{max}}, ET_0 = max\{0,\ k_{E1} 0.0018(T_{avg} + 17.8)(T_{max} - T_{min})^{0.5} R_a - k_{E2}\} \\ R + G = \bar{P}^{m_{p1}} \left(\alpha_3 \bar{W} + \left(\frac{\bar{W}}{W_{max}}\right)^{m_{w1}}\right) + \alpha_0 + \alpha_1 \bar{W} + \alpha_2 \bar{W}^{m_{w2}} \end{bmatrix}, \quad (11)$$

where,

$$\bar{P} = \begin{cases} P - P_{linf} \ \ for \ \ P > P_{linf} \\ 0 \ \ otherwise \end{cases}.$$

$$\bar{W} = \begin{cases} W - W_{linf} \ \ for\ W > W_{linf} \\ 0 \ \ otherwise \end{cases}$$

The parameters to be estimated are: k_p, W_{max}, m_{w1}, α_1, k_{E1}, k_{E2}, α_0, α_3, α_2, m_{w2} and m_{p1}.

3. Study sites, and model discretization, calibration and evaluation

3.1. Study sites and meteorological data

Three weather stations were selected for this study: Naranjal, Calarcá (CALARCA AUTOM) and Balboa (BALBOA AUTOM). The experimental Naranjal station (04°58'N, 75°39'W) is located in Chinchiná (Caldas, Colombia) at an elevation of 1381 m, with an average temperature of 20.9°C and Castillo variety coffee crop [49]. The distance between plants and rows is 1.0 by 2.0 m and the soil bulk density is 0.64 g/cm^3. The records of daily precipitation, daily maximum air temperature, daily minimum air temperature, daily average air temperature and daily average soil moisture were extracted from [49] through image digitization using WebPlotDigitizer software (https://automeris.io/WebPlotDigitizer/index.html), spanning from July 10, 2015 to December 1, 2015 (Figure A1). The soil moisture measurements correspond to 10 cm in depth.

CALARCA AUTOM (4.528°N, 75.596W) is located at Calarcá (Quindío, Colombia) at an elevation of 2255 m. The climate is cold and humid, and the land cover type is cropland and pastures [50]. The records of daily precipitation, daily maximum air temperature, daily minimum air temperature, daily average air temperature and daily average soil moisture were collected from the IDEAM database (http://www.ideam.gov.co/) and span from April 21, 2021 to October 27, 2021, including a period with no measurement from May 13, 2021 to July 26, 2021 (Figure A2). The short dataset spans from September 1, 2021 to October 27, 2021. The soil moisture measurements correspond to 10 cm in depth.

BALBOA AUTOM (2.033°N, 77.222W) is located at Balboa (Cauca, Colombia) at an elevation of 1700 m. The climate is temperate and humid, and the land cover type is cropland and pastures [50]. The records of daily precipitation, daily maximum air temperature, daily minimum air temperature, daily average air temperature and daily average soil moisture were collected from the IDEAM database (http://www.ideam.gov.co/) and span from January 01, 2019 to December 31, 2019 (Figure A3). The

soil moisture measurements correspond to 10 cm in depth.

3.2. Model discretization

The discretized form of Eq (1) is [51]:

$$W_k = W_{k-1} + \Delta_t\left(P_{ef,k} - E_k - R_k - G_k\right), \tag{12}$$

where Δ_t is the time increment, whereas $P_{ef,k}, E_k, R_k,$ and G_k are the values of $P_{ef}, E, R,$ and G at time k, given by: Eq (7) for model K7; Eq (6) for model K8; Eq (5) for model VJRAM; Eq (8) for model HDG0; Eq (10) for model HDG1; Eq (11) for model HDG3; and Eq (9) for model HDG4.

3.3. Model calibration and performance evaluation

The models, using the discretized model Eq (12) instead of the continuous time model Eq (1) are: K7 (7); K8 (6); VJRAM [Eqs (12) and (5)]; HDG0 [Eqs (12) and (8)]; HDG1 [Eqs (12) and (10)]; HDG3 [Eqs (12) and (11)]; and HDG4 [Eqs (12) and (9)]. These models are calibrated using records of daily precipitation, daily maximum air temperature, daily minimum air temperature, daily average air temperature and daily average soil moisture. An initial estimate of each parameter is chosen, and the parameter estimates are obtained by minimization of the sum of the squared deviations between the observed and simulated data, using MATLAB (The MathWorks Inc., Natick, MA, USA) with the fmin function. The fitting quality is assessed via the simulation error metrics and the Akaike information criteria. The simulation error metrics compare the observed and simulated soil moisture values over the time range (see [25,52,53]):

- Mean absolute error:

$$MAE = N^{-1}\sum\left|X_{model,j} - X_{obs,j}\right|$$

- Root-mean-square error:

$$RMSE = \sqrt{N^{-1}\sum\left(X_{model,j} - X_{obs,j}\right)^2}$$

- Mean bias error:

$$MBE = N^{-1}\sum\left(X_{model,j} - X_{obs,j}\right)$$

- Classical Nash-Sutcliffe efficiency:

$$NS_0 = 1 - \frac{\sum\left(X_{model,j} - X_{obs,j}\right)^2}{\sum\left(X_{obs,j} - \overline{X_o}\right)^2}$$

- Nash-Sutcliffe efficiency based on absolute error:

$$NS_{abs} = 1 - \frac{\sum\left|X_{model,j} - X_{obs,j}\right|}{\sum\left|X_{obs,j} - \overline{X_o}\right|}$$

The term $X_{obs,j}$ represents the observed values, $X_{model,j}$ represents the simulated values, $\overline{X_o}$

represents the mean of observed values, N represents the number of observations and the summation Σ holds over the range of the time series. The Nash-Sutcliffe (NS) coefficient ranges between $-\infty$ and 1.0; an NS value of 1.0 corresponds to perfect fit, 0.0 corresponds to a model that is not better than using the average value and a negative value corresponds to a model that has less efficacy than the mean of the observations [25,54]. The range $NS > 0.7$ is considered as satisfactory fitting by some authors, whereas $NS \geq 0.8$ is considered as high fitting quality [23,53], but there is no universally accepted criterion [25,28]. Low values of MAE, RMSE and MBE correspond to high fitting quality [53].

In addition, the Akaike information criterion allows comparison of models considering both the prediction quality and the number of model parameters. The basic Akaike information criterion is [55–57]:

$$AIC = N \ln\left(\frac{SSE}{N}\right) + 2(N_p + 1),$$

where SSE is the sum of squared errors, N is the number of observations and N_p is the number of parameters of a given model. The Akaike information criteria for the case that the number of observations is small in comparison to the number of parameters $N_p + 1$, that is, $N_p > N/40$, is [55–57]:

$$AIC_c = N \ln\left(\frac{SSE}{N}\right) + 2(N_p + 1) + \frac{2(N_p+1)(N_p+2)}{N-N_p-2} = N \ln\left(\frac{SSE}{N}\right) + \frac{2N(N_p+1)}{N-N_p-2}.$$

The best model is the one with the lowest AIC value [56,57]. In addition, the effect of model parameters on the weighted sum of squared simulation errors (E) allows identification of which parameters require an accurate estimation [53], E being given by:

$$E = \sum \frac{\left(X_{model,j} - X_{obs,j}\right)^2}{\left(\max\left(X_{obs,j}\right)\right)^2}$$

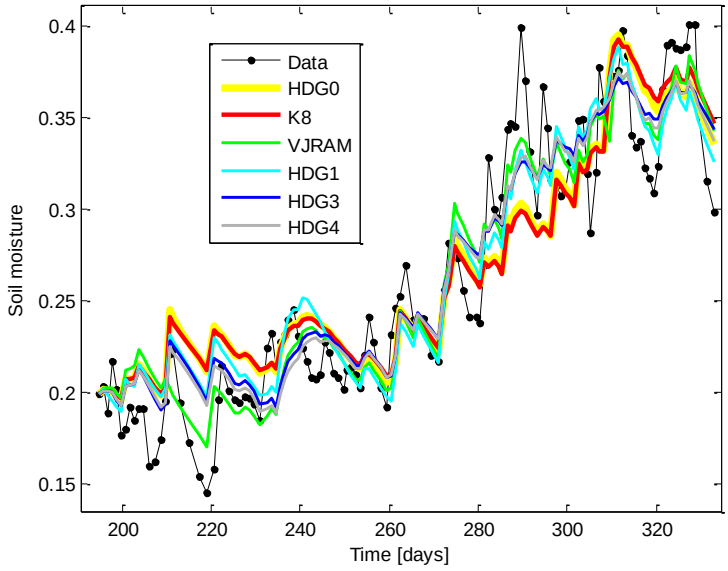

Figure 1. Predicted and observed soil moisture at the Naranjal station, period $\Omega_{N123} = [194 - 333]$.

4. Model fitting results

The predicted and observed soil moisture data for the Naranjal station, period $\Omega_{N123} = [194 - 333]$ are shown in Figure 1. The values of performance criteria are given in Table 3. The sensitivity analysis is shown in Figure 5.

Table 3. Performance of soil moisture models at the Naranjal station. Periods: $\Omega_{N123} = [194 - 333]$, $\Omega_{N13} = [194 - 264] \cup [310 - 333]$ and $\Omega_{N2} = [265 - 309]$.

Calibration /validation	Model	MAE	RMSE	MBE	NS_{abs}	NS_0	AIC
Calibration over Ω_{N123}	K7	0.0238	0.0305	-0.0039	0.6246	0.8165	-857.8970
	K8	0.0238	0.0305	-0.0037	0.6242	0.8163	-857.7440
	VJRAM	0.0190	0.0231	-0.0014	0.7001	0.8949	**-925.2461**
	HDG0	0.0238	0.0299	-0.0040	0.6246	0.8227	-862.1540
	HDG1	0.0205	0.0255	-0.0034	0.6764	0.8712	-895.1604
	HDG3	0.0197	0.0244	-0.0034	0.6897	0.8827	-901.9908
	HDG4	0.0190	0.0237	-0.0030	0.7000	0.8892	-901.5107
Calibration over Ω_{N13}	VJRAM	0.0176	0.0215	-0.0032	0.7071	0.9122	-626.8587
Validation over Ω_{N2}	VJRAM	0.0217	0.0286	-0.0105	0.4544	0.6338	-270.8257

The boxplot for soil moisture models for Naranjal station is given in Figure 2, and the Taylor diagram is given in Figure 3.

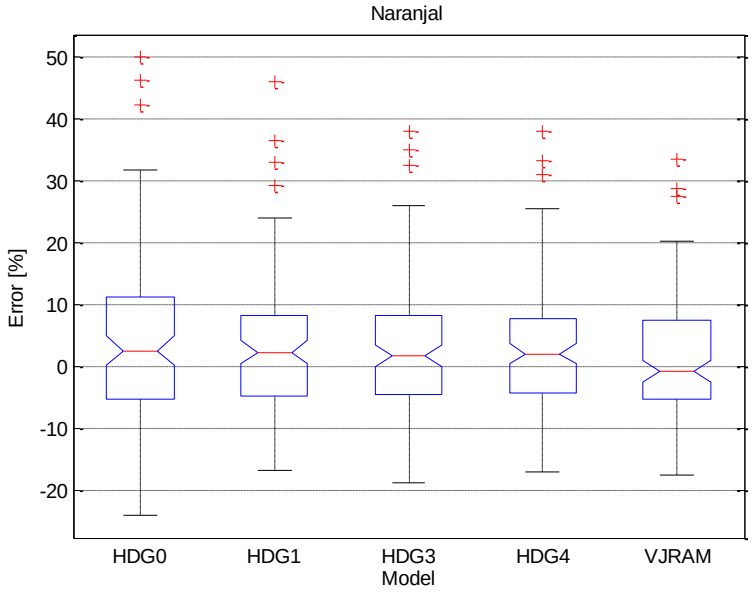

Figure 2. Error percentage for soil moisture modelling for Naranjal station, period Ω_{N123}.

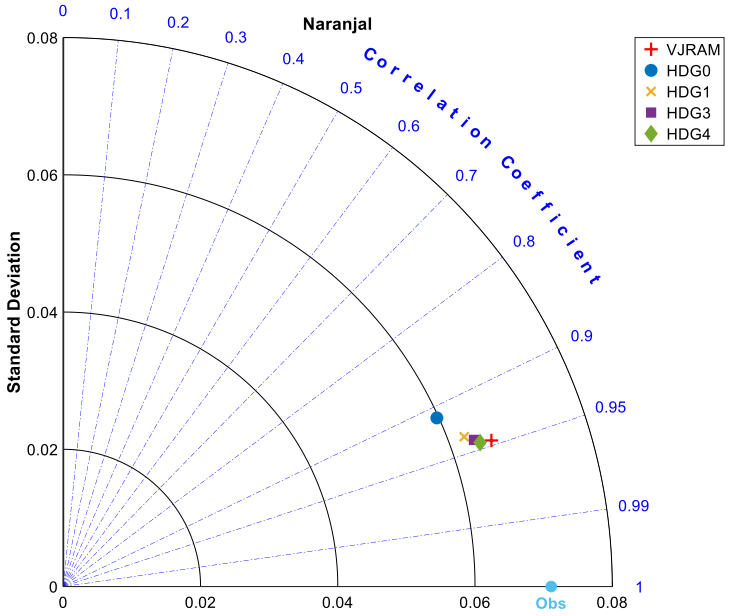

Figure 3. Taylor diagram of the simulated soil moisture for Naranjal station.

The order of the models, from the lowest to the highest AIC, the lowest to the highest RMSE and the highest to the lowest NS_0, is:

- AIC: VJRAM, HDG3, HDG4, HDG1, HDG0, K7, K8.
- RMSE: VJRAM, HDG4, HDG3, HDG1, HDG0, K7, K8.
- NS_0: VJRAM, HDG4, HDG3, HDG1, HDG0, K7, K8.

Therefore, the order of models is different for the AIC, RMSE and NS_0 indices, but VJRAM model is the best according to AIC, RMSE and NS_0, whereas models HDG3 and HDG4 achieve either the second or third place. The second lowest AIC corresponds to HDG3 and the second highest NS_0 (0.889) corresponds to the HDG4 model. The NS_0 values obtained with the K7 and K8 models (in the range 0.816–0.817) are lower than those of the HDG models (range 0.822–0.890). The boxplot (see Figure 2) indicates that: i) HDG3, HDG4 and VJRAM models have a similar interquartile range (IQR), lower than that of HDG0 and HDG1; ii) VJRAM model has the lowest range and the lowest median; iii) HDG0 model has the highest IQR, the highest range and the highest outliers. The Taylor diagram (see Figure 3) indicates that: i) the correlation coefficient (R) is higher than 0.9 for the models, so that the modelling data are similar to measurement data; ii) VJRAM and HDG4 models have higher correlation coefficient, whereas HDG0 has the lowest value. Finally, the VJRAM model Eq (5) is chosen as the highest quality model, and the main reason is that it has the lowest AIC and the highest NS_0. The better performance of VJRAM model confirms the effectiveness of the tailored structure of percolation term G for improved soil moisture modelling. The predicted and observed soil moisture values for the Naranjal station, using the VJRAM model are shown in Figure 4.

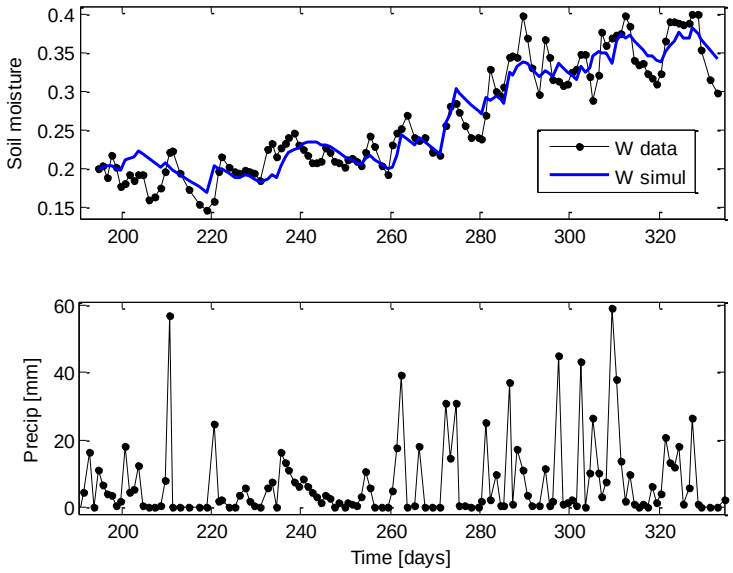

Figure 4. Predicted and observed soil moisture at the Naranjal station, using the VJRAM model, period $\Omega_{N123} = [194 - 333]$.

The sensitivity analysis for the VJRAM model (Naranjal station) is shown in Figure 5.

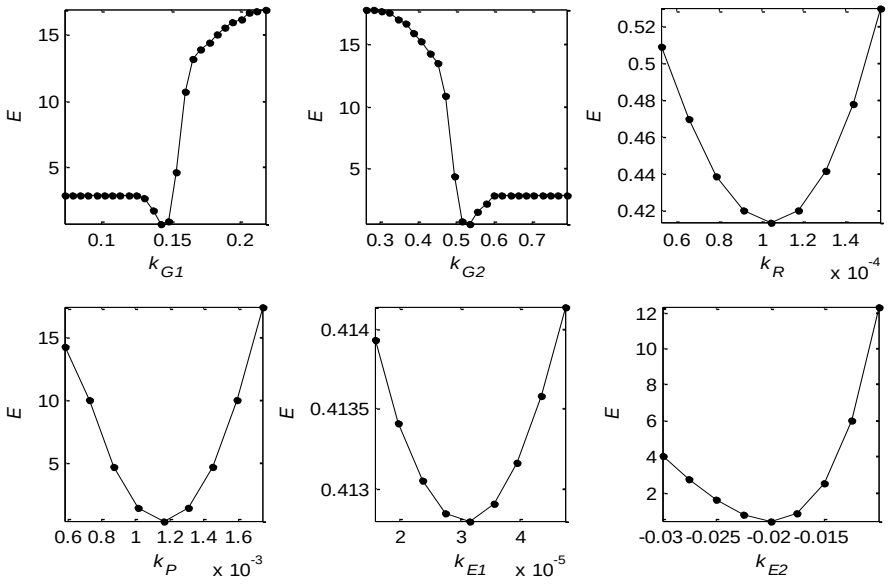

Figure 5. Sensitivity analysis for the VJRAM model at the Naranjal station.

The effects of model parameters on model fit for the Naranjal station are: i) higher effect: k_{G1}, k_{G2}, k_P and k_{E2}; ii) lower effect: k_R and k_{E1}. Therefore, accurate estimation of k_{G1}, k_{G2}, k_P and k_{E2} is important.

Collecting additional meteorological records for Naranjal station is not straightforward, and there is not a public database with this information. Therefore, the 2015 period $\Omega_{N123} = [194 - 333]$ is split into calibration period $\Omega_{N13} = [194 - 264] \cup [310 - 333]$ and validation period $\Omega_{N2} =$

$[265-309]$. Then, model VJRAM is calibrated over Ω_{N13} and the obtained parameter estimates are used for model validation over period Ω_{N2}. The error metrics are given in Table 3; the simulations of soil moisture over time for calibration and validation periods are given in Figure 6; the plots of measurements versus simulation (calibration and validation) are given in Figure 7.

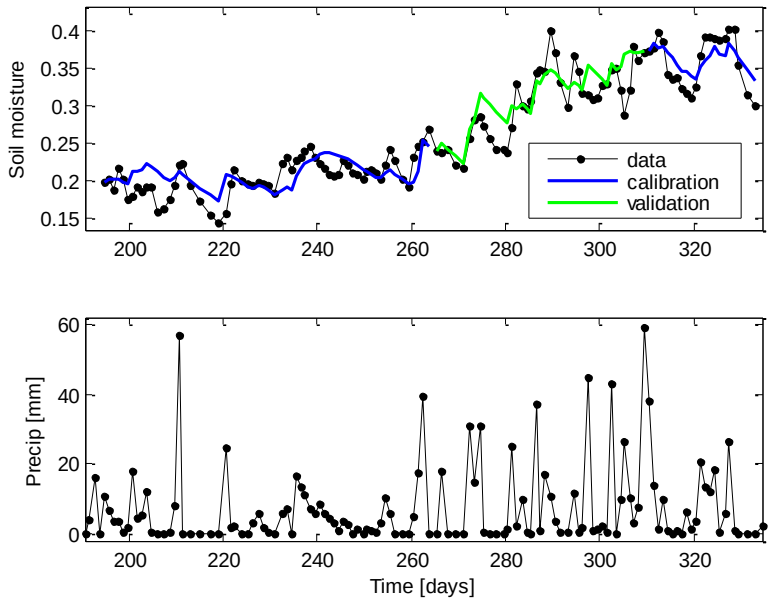

Figure 6. Calibration and validation of VJRAM model at Naranjal station, for calibration period Ω_{N13} and validation period Ω_{N2}.

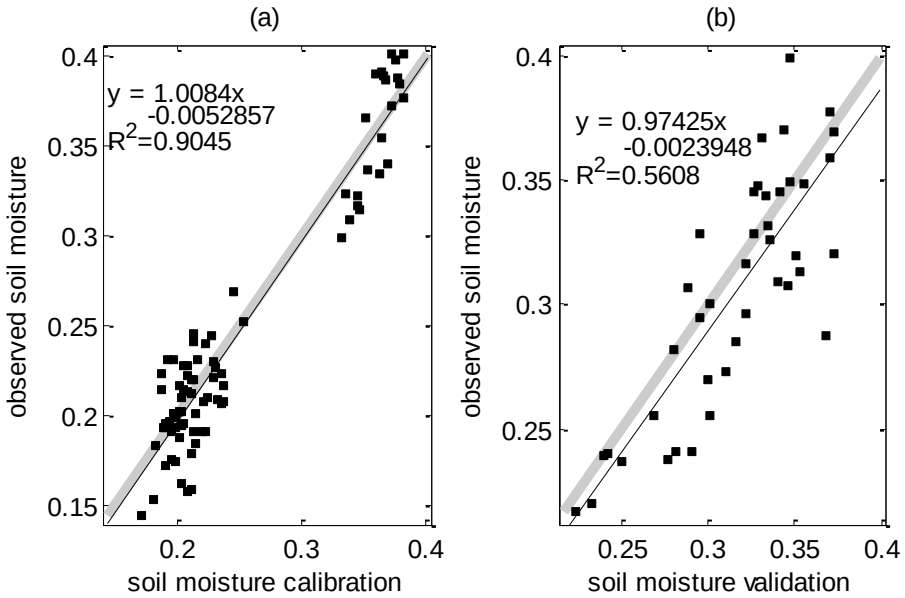

Figure 7. Measured versus simulated soil moisture for Naranjal station, using VJRAM model: (a) calibration period Ω_{N13}, (b) validation period Ω_{N2}.

The predicted and observed soil moisture data for the Calarcá station over period $\Omega_{K3} = [244-300]$ are shown in Figure 8; the values of performance criteria are given in Table 4.

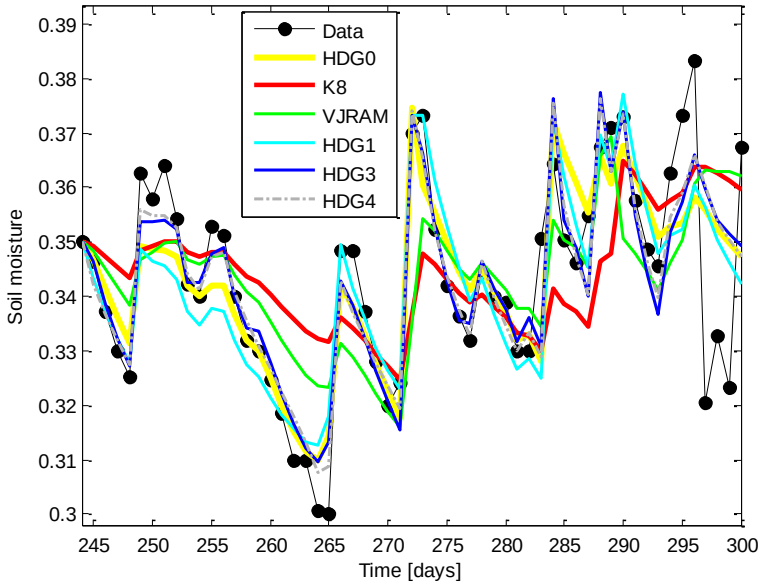

Figure 8. Predicted and observed soil moisture at the Calarcá station, for period $\Omega_{K3} = [244 - 300]$.

Table 4. Performance of soil moisture models at Calarcá station. Periods: $\Omega_{K3} = [244 - 300]$ days; $\Omega_{K123} = [111 - 132] \cup [208 - 235] \cup [244 - 300]$ days; $\Omega_{K13} = [111 - 132] \cup [244 - 300]$ days; $\Omega_{K2} = [208 - 235]$ days.

Calibration /validation	Model	MAE	RMSE	MBE	NS_{abs}	NS_0	AIC
Calibration over $\boldsymbol{\Omega_3}$	K7	0.0132	0.0167	-0.0008	0.1409	0.2101	-450.0530
	K8	0.0130	0.0165	-0.0011	0.1519	0.2302	-451.5170
	VJRAM	0.0115	0.0150	-0.0003	0.2508	0.3680	-460.0512
	HDG0	0.0080	0.0111	-0.0001	0.4768	0.6532	-496.9674
	HDG1	0.0073	0.0108	0.0002	0.5206	0.6684	-491.0250
	HDG3	0.0068	0.0101	0.0000	0.5579	0.7113	**-492.6095**
	HDG4	0.0066	0.0101	0.0001	0.5709	0.7120	-482.1478
Calibration over $\boldsymbol{\Omega_{123}}$	HDG3	0.0069	0.0108	0.0004	0.6855	0.8401	
Calibration over $\boldsymbol{\Omega_{13}}$	HDG3	0.0066	0.0104	$-1x10^{-6}$	0.6677	0.8350	-692.1198
Validation over $\boldsymbol{\Omega_2}$	HDG3	0.010621	0.015766	-0.0096	0.57833	0.68457	-187.5935

The boxplot for soil moisture models for Calarcá station is given in Figure 9, and the Taylor diagram is given in Figure 10.

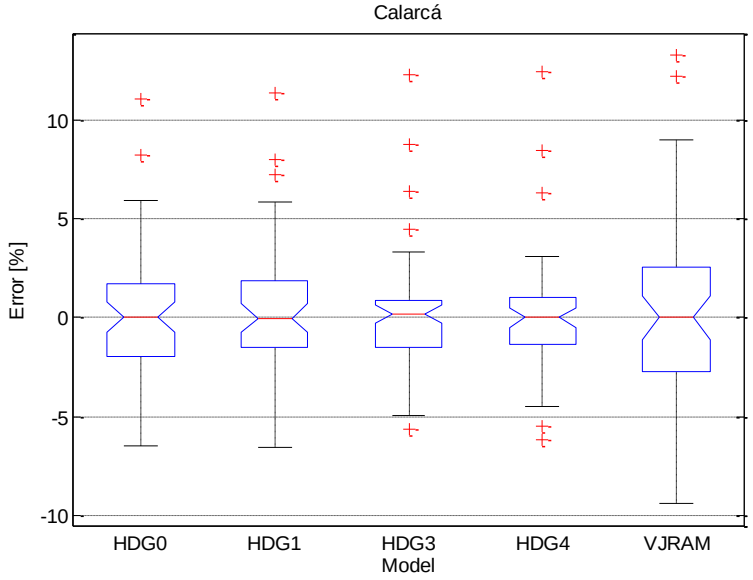

Figure 9. Error percentage for soil moisture modelling for Calarcá station, period Ω_{K3}.

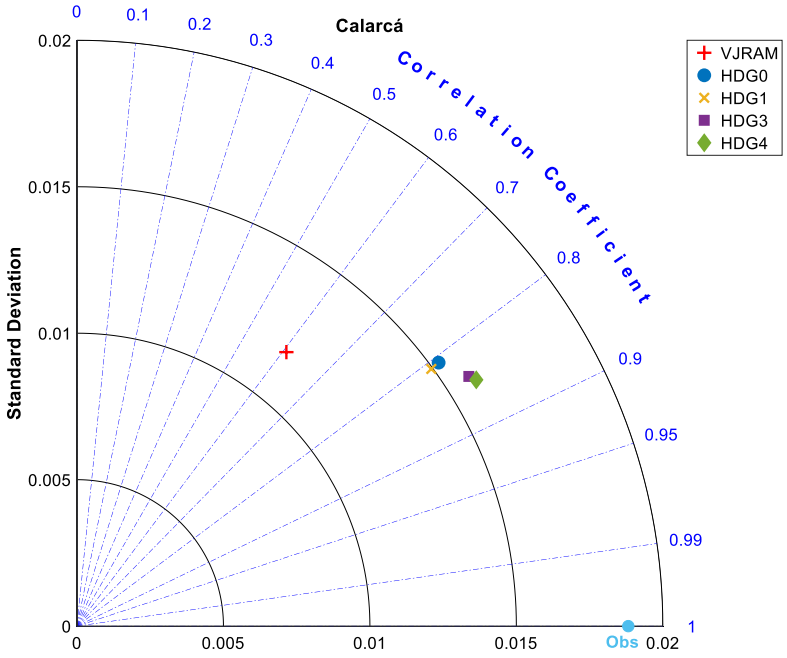

Figure 10. Taylor diagram of the simulated soil moisture for Calarcá station.

The NS_0 values obtained with K7, K8 and VJRAM models are in the range 0.21–0.37, whereas the NS_0 values for HDG models are in the range 0.653–0.712. The order of the models, from the lowest to the highest AIC, the lowest to the highest RMSE and the highest to the lowest NS_0 is:

-AIC: HDG0, HDG3, HDG1, HDG4, VJRAM, K8, K7.
-RMSE: HDG3 and HDG4 (same value), HDG1, HDG0, VJRAM, K8, K7.
-NS_0: HDG4, HDG3, HDG1, HDG0, VJRAM, K8, K7.

Therefore, HDG3 model achieves either the first or second place in the RMSE and NS_0 indices, whereas HDG4 model achieves the highest NS_0 but it is in the fourth place in terms of AIC. The boxplot (see Figure 9) indicates that: i) all the models have a near-zero median; ii) HDG4 and HDG3 models have a similar IQR and range; iii) HDG4 model has the lowest range, whereas HDG4 and HDG3 have the lowest IQR; iv) VJRAM model has the highest range, the highest IQR and the highest outliers. In summary, HDG4 and HDG3 are the best two models in terms of range and IQR, whereas VJRAM is the worst model. The Taylor diagram (see Figure 10) indicates that: i) for the VJRAM model, the correlation coefficient (R) is close to 0.6 (see Figure 10), while other models (HDG0, HDG1, HDG3, HDG4) have an R higher than 0.8; ii) The HDG3 and HDG4 models have a similar R, and the HDG4 model has the highest R. Finally, the HDG3 model is chosen as the highest quality model, and the main reason is that the lowest AIC corresponds to HDG0, but its NS_0 (0.6532) is lower than 0.7, whereas HDG3 has the second lowest AIC and exhibits $NS_0 > 0.7$. Then, the HDG3 model is fitted using the period $\Omega_{K123} = [111-132]\cup[208-235]\cup[244-300]$. The resulting predicted and observed soil moisture values are shown in Figure 11, and the performance is:

MAE: 0.0069431; RMSE: 0.010809; MBE: 0.00036298; NS_{abs}: 0.68547; and NS_0: 0.84014.

It achieves a high simulation capability for low (0.27–0.30) and high (0.36–0.38) soil moisture ranges and for the drying time periods after rain events.

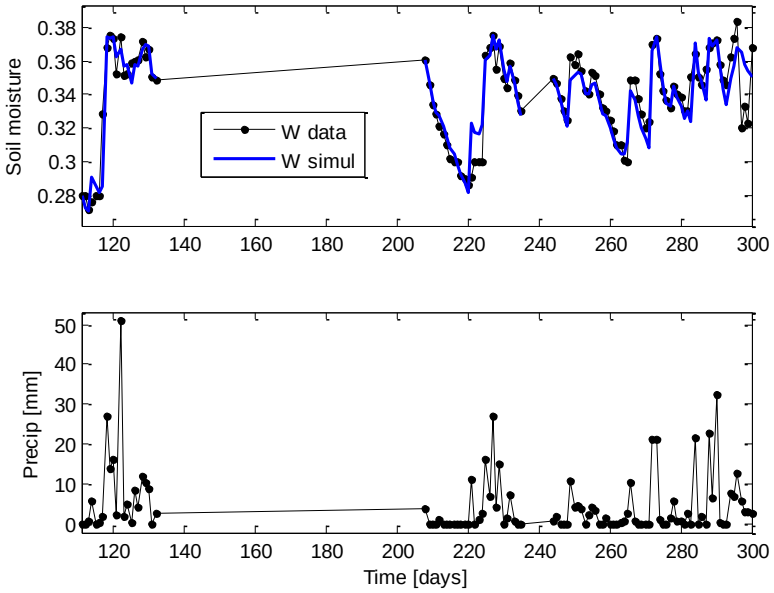

Figure 11. Predicted and observed soil moisture at Calarcá station, using the HDG3 model, for period $\Omega_{K123} = [111-132]\cup[208-235]\cup[244-300]$days.

The sensitivity analysis for the HDG0 model (Calarcá station) is shown in Figure 12.

The effect of model parameters on model fit for the Calarcá station is: i) higher effect: m, k_p and W_{max}; ii) lower effect: α, k_{E2} and k_{E1}. Therefore, an accurate estimation of m, k_p and W_{max} is important.

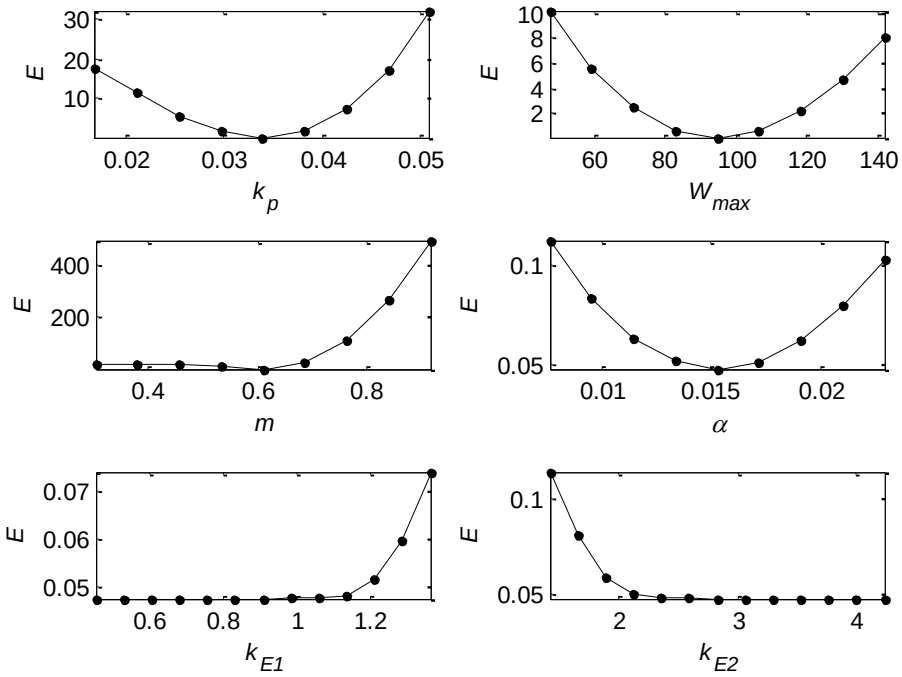

Figure 12. Sensitivity analysis for the HDG0 model at the Calarcá station.

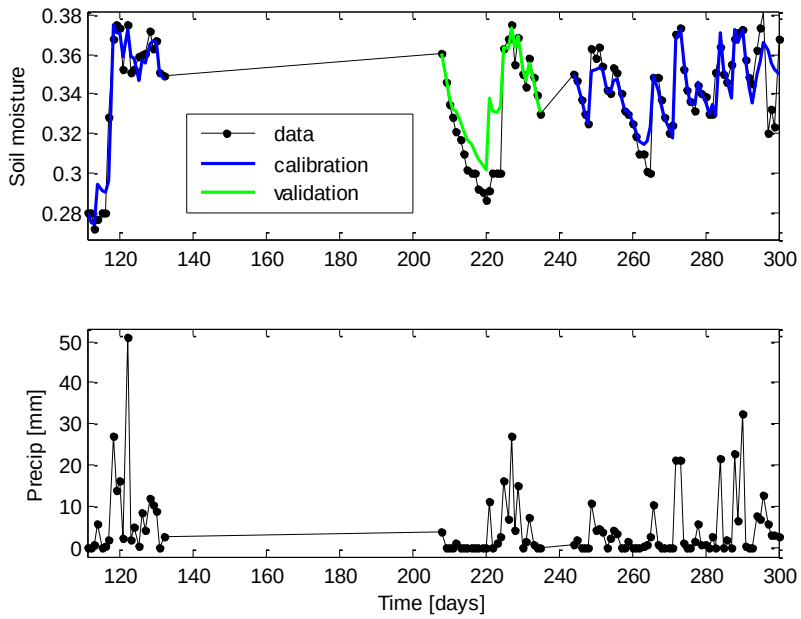

Figure 13. Simulation of soil moisture at Calarcá station using HDG3 model, for calibration period $\Omega_{K13} = [111 - 132] \cup [244 - 300]$ and validation period $\Omega_{K2} = [208 - 235]$.

Model validation for Calarcá station over 2020 or 2022 is hampered by the quality of meteorological data: corresponding daily measurements of precipitation, average temperature, maximum temperature, minimum temperature and soil moisture over time periods of at least 50 days, in 2020 or 2022 are not available from the IDEAM database. Therefore, the year 2021 is split into calibration period $\Omega_{K13} = [111 - 132] \cup [244 - 300]$ and validation period $\Omega_{K2} = [208 - 235]$. Then, model HDG3 is calibrated over Ω_{K13}, and the obtained parameter estimates are used for model

validation over period Ω_{K2}. The error metrics are given in Table 4; the calibration and validation of soil moisture over time are given in Figure 13; the plots of measurements versus simulation (calibration and validation) are given in Figure 14.

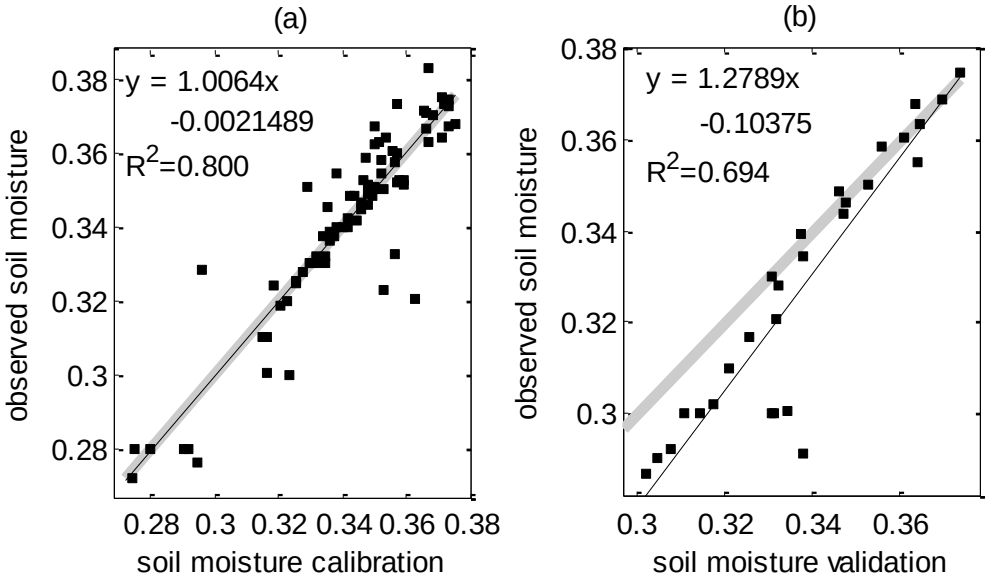

Figure 14. Measured versus simulated soil moisture for Calarcá station, using HDG3 model, for (a) calibration period Ω_{K13}, (b) validation period Ω_{K2}.

For Balboa station, soil moisture models are calibrated over Ω_{B1}=[1−318] ∪ [321−365], 2019, and the obtained parameter estimates are used for model validation over period Ω_{B2}=[01−129], 2020. The simulations of soil moisture for period Ω_{B1} are shown in Figure 15. The values of the performance criteria are given in Table 5.

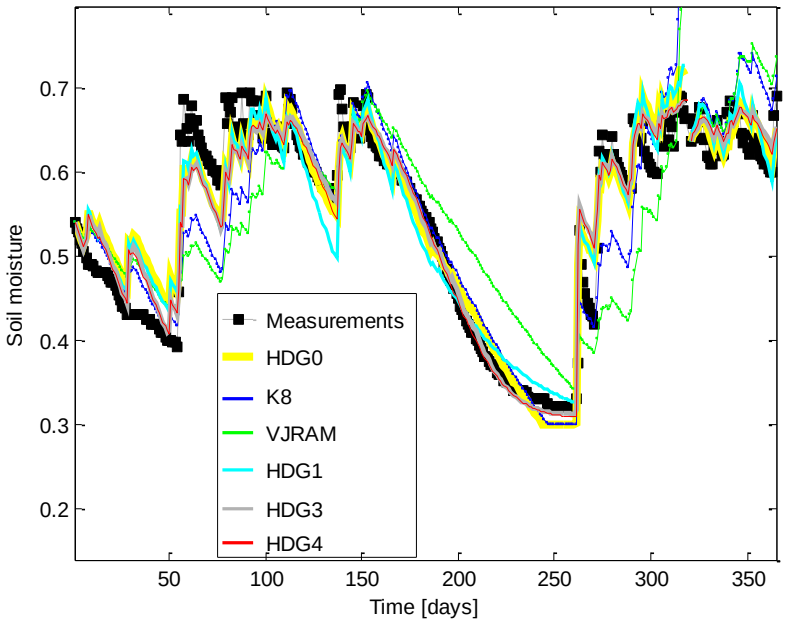

Figure 15. Predicted and observed soil moisture at the Balboa station, for period Ω_{B1}.

Table 5. Performance of soil moisture models at the Balboa station.

Calibration /validation	Model	MAE	RMSE	MBE	NS_{abs}	NS_0	AIC
Calibration, period $\boldsymbol{\Omega_{B1}}$	K7	0.024716	0.043898	0.00070779	0.81542	0.95087	-3961.9446
	K8	0.025297	0.044969	0.00076823	0.81109	0.94845	-3931.2820
	VJRAM	0.038119	0.062076	-0.0000454	0.7153	0.90176	-3519.1533
	HDG0	0.015477	0.026016	-0.0010581	0.88442	0.98275	**-4627.4205**
	HDG1	0.016412	0.027174	-0.0025826	0.87744	0.98117	-4565.8392
	HDG3	0.023413	0.032755	-0.0024922	0.77449	0.92158	-2457.0807
	HDG4	0.022738	0.031992	-0.0026534	0.78099	0.92519	-2467.6931
Validation, period $\boldsymbol{\Omega_{B2}}$	HDG0	0.020127	0.023863	-0.007264	0.33591	0.5912	-948.8152

The boxplot for soil moisture models for Balboa station is given in Figure 16, and the Taylor diagram is given in Figure 17.

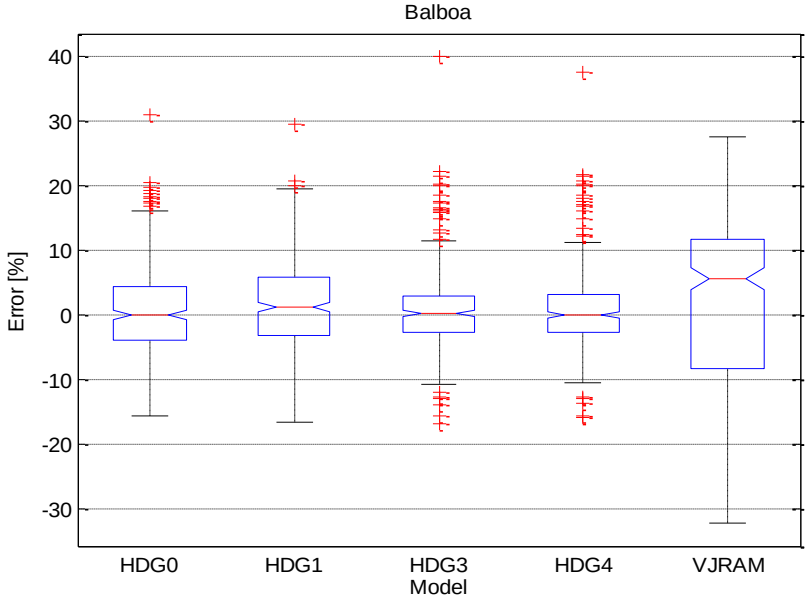

Figure 16. Error percentage for soil moisture modelling for Balboa station, period Ω_{B1}.

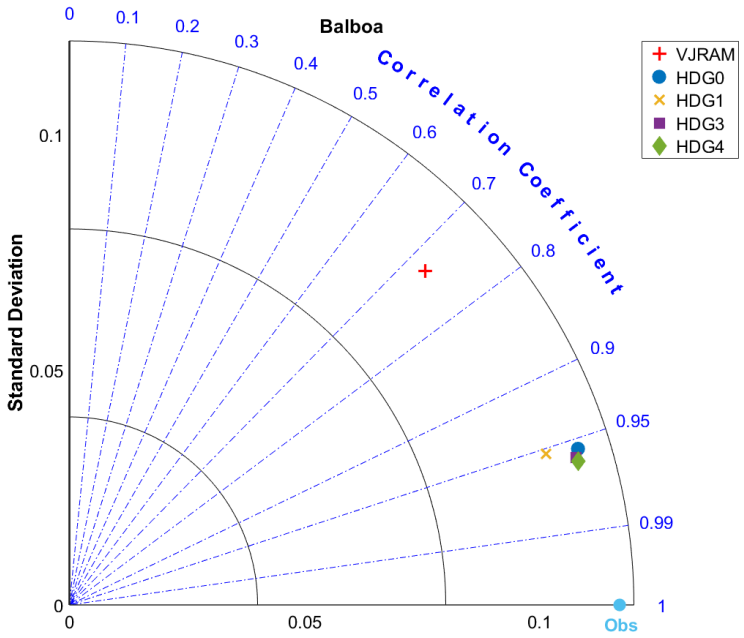

Figure 17. Taylor diagram of the simulated soil moisture for Balboa station.

The order of the models, from the lowest to the highest AIC, the lowest to the highest RMSE and the highest to the lowest NS_0 is:

-AIC: HDG0, HDG1, K7, K8, VJRAM, HDG4, HDG3.
-RMSE: HDG0, HDG1, HDG4, HDG3, K7, K8, VJRAM.
-NS_0: HDG0, HDG1, K7, K8, HDG4, HDG3, VJRAM.

Therefore, the HDG0 model is the best one according to AIC, RMSE and NS_0, whereas the HDG1 model is the second best. The NS_0 values obtained with the K7 and K8 models (in the range 0.948–0.951) are comparable to those of the HDG models (range 0.921–0.983). The NS_0 value for the VJRAM model (0.902) is the lowest. The boxplot (Figure 16) indicates that: i) HDG0, HDG3 and HDG4 models have a near zero median; ii) HDG3 and HDG4 models have the lowest range and the lowest IQR (see Figure 16), but their disadvantage is the higher amount of outliers compared to other models; iii) VJRAM model has the highest range, the highest IQR and the highest median; iv) HDG0 model has a lower amount of outliers compared to HDG3 and HDG4 models, although its IQR and range are higher. The Taylor diagram (see Figure 17) indicates that: i) all the correlation coefficients (R) are higher than 0.7, the R of VJRAM is close to 0.73 and the R of other models is close to 0.95; ii) the R of HDG0, HDG1, HDG3 and HDG4 is similar, and it is higher than that of VJRAM. Finally, the HDG0 model is chosen as the highest quality model, and the main reason is that it has the lowest AIC (-4627.4) and the highest NS_0 (0.983). The predicted and observed soil moisture values for Balboa station, using the HDG0 model are shown in Figure 18.

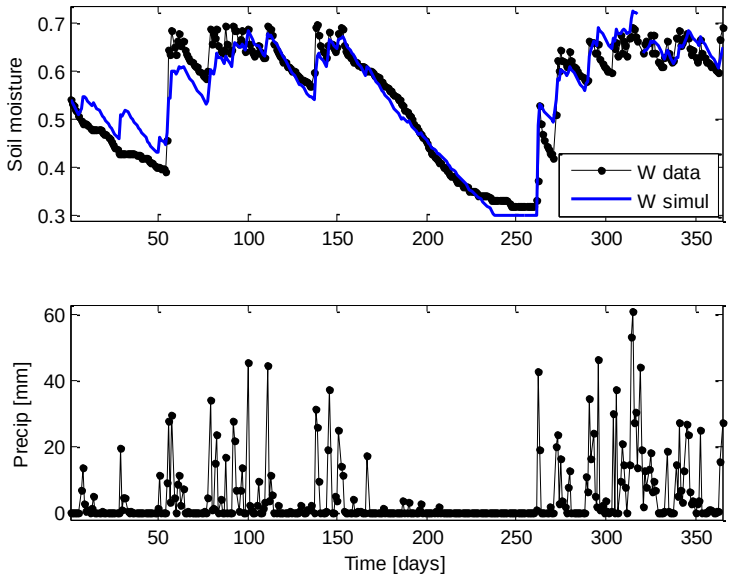

Figure 18. Predicted and observed soil moisture at the Balboa station, using the HDG0 model, for period Ω_{B1}.

The sensitivity analysis for the HDG0 model (Balboa station) is shown in Figure 19.

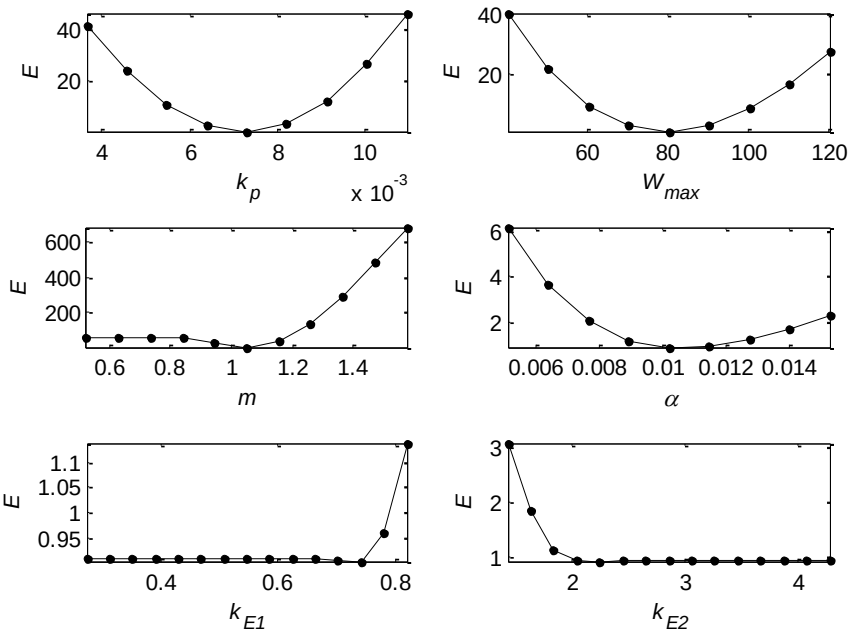

Figure 19. Sensitivity analysis for the HDG0 model at the Balboa station.

The effect of model parameters on model fit for Balboa station is: i) higher effect: m, k_p and W_{max}; ii) lower effect: α, k_{E2} and k_{E1}. Therefore, an accurate estimation of m, k_p and W_{max} is important.

Model HDG0 is validated for Balboa station, period Ω_{B2}=[01 − 129], 2020, using estimated parameters obtained from calibration. The error metrics are given in Table 5; the simulation of soil

moisture over time for validation period is given in Figure 20; the plots of measurements versus simulation (calibration and validation) are given in Figure 21.

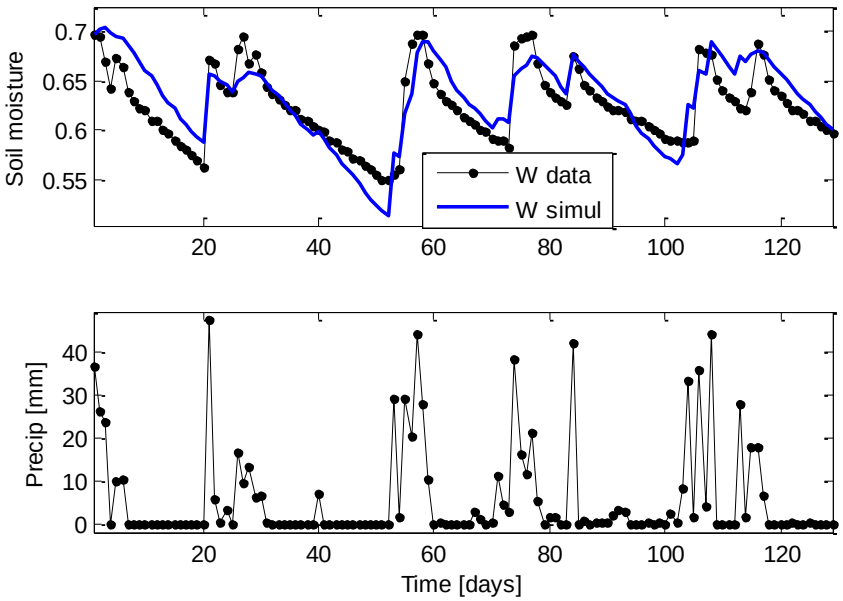

Figure 20. Simulation of soil moisture at Balboa station using HDG0 model for validation period Ω_{B2}.

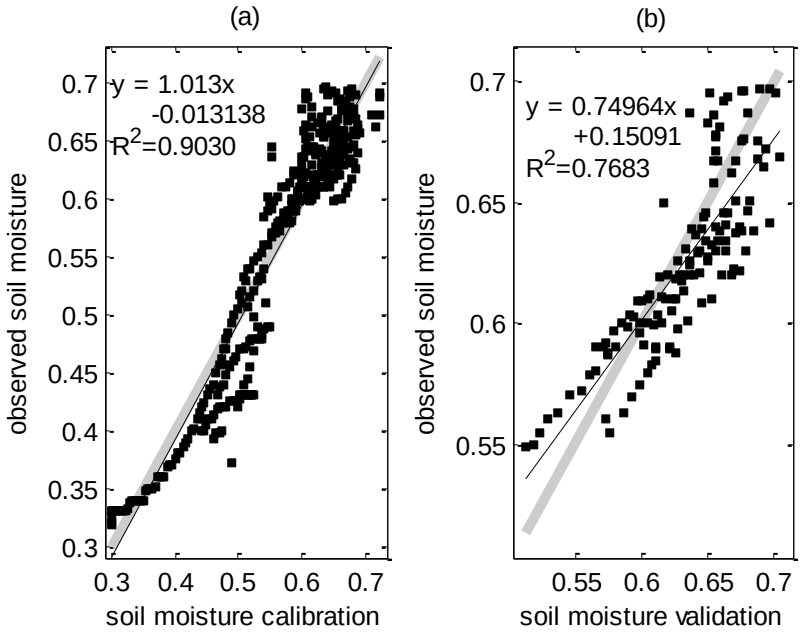

Figure 21. Measured versus simulated soil moisture for Balboa station, using the HDG0 model, for (a) calibration period Ω_{B1} and (b) validation period Ω_{B2}.

Table 6. Models with the highest NS_0 (first and second highest NS_0) and the lowest AIC (first and second lowest AIC), for calibration.

Site	Model with the first and second highest NS_0 value {and number of parameters}	Models with the first and second lowest AIC value
Naranjal	VJRAM {7}	VJRAM,
	HDG4 {14}	HDG3
Calarcá	HDG4 {14},	HDG0,
	HDG3 {11}	HDG3
Balboa	HDG0 {6},	HDG0,
	HDG1 {9}	HDG1

The parameter values of the models with best performance are given in Table 7.

Table 7. Parameter values of the models with best performance for the three stations.

Site	Model	Parameters
Naranjal	VJRAM	$k_p = 0.0011591,\ k_{E1} = 3.4494 \times 10^{-5},\ k_{E2} = -0.01999,$ $k_{R1} = 9.6023 \times 10^{-5},\ k_{G1} = 0.14761,\ k_{G2} = 0.53393,$ $k_{R2} = 0.00055726.$
Calarcá	HDG3	$k_p = 0.012728,\ W_{max} = 4004.6595,\ m_{w1}$ =0.88719, $\alpha_1 = 6.4902,\ k_{E1} = 5.5575,\ k_{E2} = 0.0085038,\ \alpha_0 = 0.24682,$ α_3=0.023991, $\alpha_2 = -5.8671,\ m_{w2} = 0.83141,\ m_{p1} = 1.084.$
Balboa	HDG0	$k_p = 0.007305,\ W_{max}$ =80.03, $m = 1.051,\ \alpha = 0.0102,\ k_{E1} = 0.5463,\ k_{E2} = 2.852.$
	HDG1	$k_{p1} = 0.6318,\ k_{p2} = 118.81,\ P_p = 1.2,\ W_{max} = 49.514,\ m = 1.188,\ \alpha = 0.02335,\ n = 0.93186,\ k_{E1}$=1.1256, $k_{E2} = 4.641.$

There is not a single model that exhibits neither the highest nor the lowest capacity for representing the soil moisture over the three stations (see Table 6). This is related to the different soil conditions. The lowest AIC values (-927.4, -496.97 and -4627.4) correspond to the VJRAM, HDG0 and HDG0 models for the Naranjal, Calarcá and Balboa stations, respectively. The highest AIC values (-857.74, -450.05 and -2457.1) correspond to the K8, K7 and HDG3 models, for the Naranjal, Calarcá and Balboa stations, respectively. In general terms, the compartment-based models (K models) exhibited worse performance compared with the HDG models: the K models exhibited neither the best NS_0 nor the best AIC value, for any of the three stations. In addition, the K7 and K8 models exhibited lower NS_0 and higher AIC compared to the HDG models. Although the HDG0 is a standard SM model, it was the best model only for the Balboa station, if both AIC and NS_0 are considered. For instance, the highest NS_0 value for the Calarcá station was obtained by the HDG4 model but the lowest AIC was obtained by the HDG0 model. This implies that HDG4 achieves higher simulation accuracy at the cost of a significantly higher number of model parameters, for the Calarcá station. For the Naranjal station, the previous knowledge on percolation representation resulted in higher capacity for modeling SM, since the VJRAM model achieved the lowest AIC and highest NS_0, by using logarithmic type nonlinear functions.

The Nash-Sutcliffe coefficient obtained was higher than 0.8 for the three stations, considering the large dataset for the Calarcá station. NS_0 values for each model depend on the weather station considered. The highest NS_0 values (0.895, 0.712 and 0.983) correspond to the VJRAM, HDG4 and HDG0 models, for the Naranjal, Calarcá and Balboa stations, respectively. These values can be considered as satisfactory, considering the complex effects of the soil that support the variation of soil moisture and the lack of measurements of relative humidity, solar radiation and wind speed. The lowest NS_0 values correspond to the K8, K7 and VJRAM models, for the Naranjal, Calarcá and Balboa stations, respectively. The NS_0 range obtained at the Balboa station (0.902 to 0.983) was higher than the NS_0 value for the Calarcá station (0.840) and the NS_0 range for the Naranjal station (0.816 to 0.895). The HDG group of models exhibited high NS_0 values for all cases. The NS_0 values for the K7 and K8 models are similar, when comparing them for the same station. For the Naranjal station, VJRAM was chosen as the best model, but the HDG4 model also exhibited a high performance, as its NS_0 (0.889) is comparable to VJRAM (0.895). The use of a combination of polynomial terms of precipitation and soil moisture resulted in better NS_0 of the HDG3 model compared to that of HDG0 for the Naranjal and Calarcá stations. However, the NS_0 of the HDG3 model was lower compared to HDG0 for the Balboa station. The main differences between the HDG3 and HDG0 models is that HDG3 includes $\alpha_3\bar{P}^{m_{p1}}\bar{W}+\alpha_0+\alpha_2\bar{W}^{m_{w2}}$ and uses $\bar{P}$ and $\bar{W}$ instead of P and W, in the $R+G$ term.

The simulated versus observed soil moisture values are given in Figure 10. The gray straight line is the identity line, and the black straight line is the linear regression.

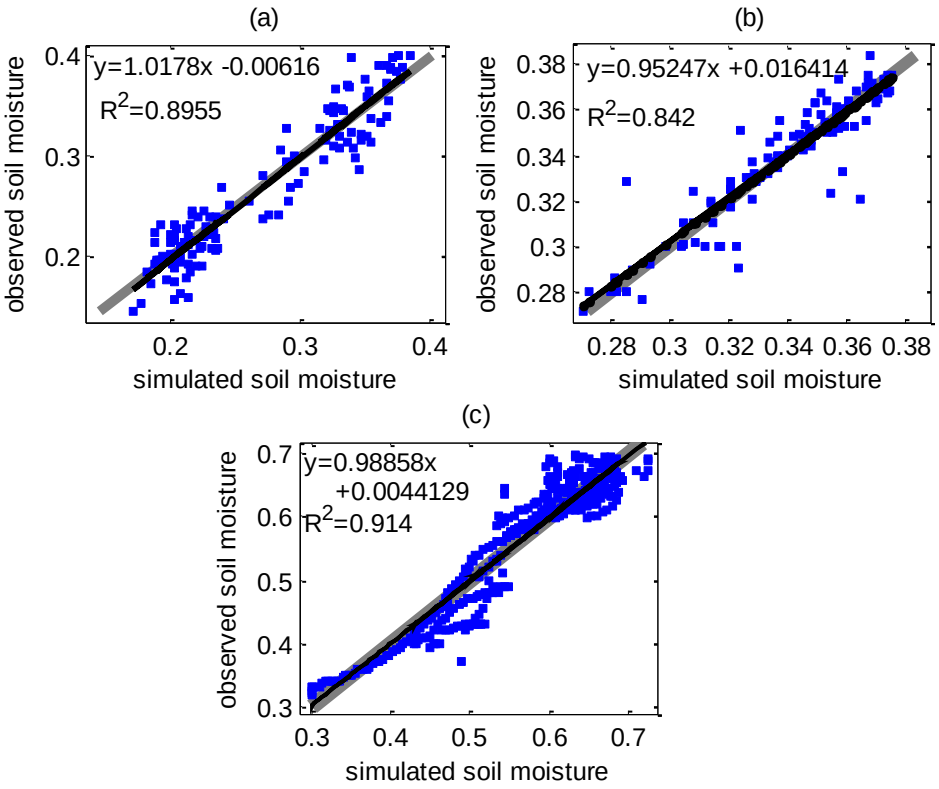

Figure 22. Simulated versus measured soil moisture values for: a) Naranjal station (VJRAM model); b) Calarcá station (HDG3 model, large dataset); and c) Balboa (HDG0 model).

The slope is similar to 1 for the three stations, which implies model consistency. The R^2 value is higher than 0.8 for the three stations, implying that a large proportion of the variation in observed values is explained by the regression model. The simulation residual versus simulated soil moisture

values are shown in Figure 11.

For the Naranjal station, there are no clear patterns, and the distribution is approximately symmetrical. For the Calarcá station, there are no clear patterns, but the residuals are shorter for the simulated SM range 0.295–0.310. For the Balboa station, the residuals are shorter and there is a nonlinear pattern for simulated SM lower than 0.42. This means that the model can be further improved.

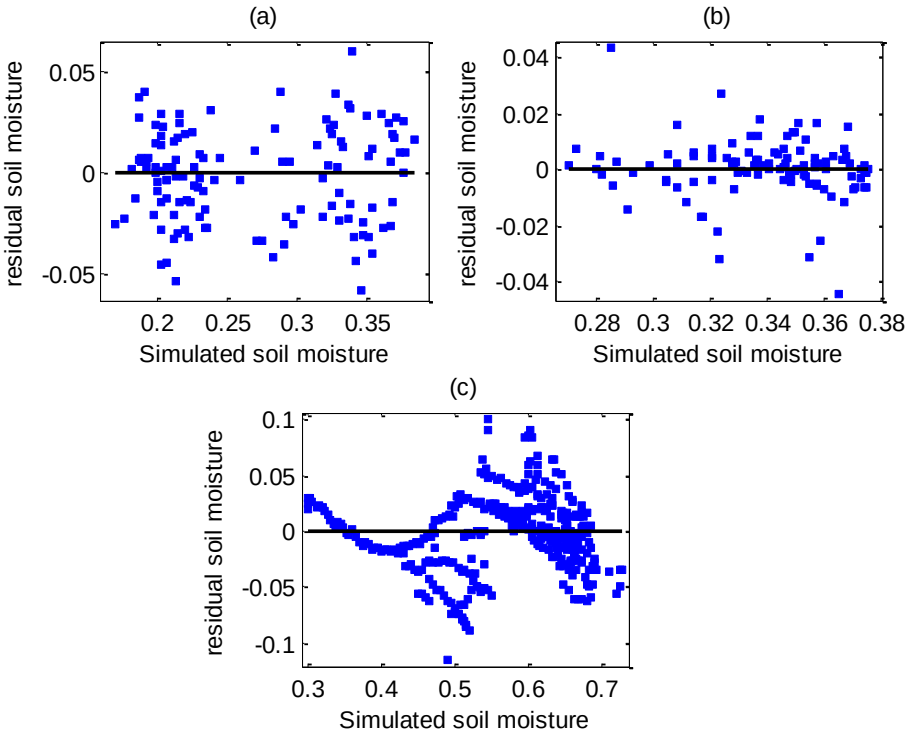

Figure 23. Residual plot of the modeled soil moisture for: a) Naranjal station (VJRAM model); b) Calarcá station (HDG3 model, large dataset); and c) Balboa (HDG0 model).

5. Discussion

The mass balance models VJRAM, HDG0, HDG3 and HDG4 are simple, as they only require basic meteorological data and no soil information. Despite the model simplicity, the obtained NS_0 and NS_{abs} values are quite high. The results confirm that alternative simple evapotranspiration equation (4) can be used for different soil conditions instead of the classical FAO56 equation, despite the high complexity of the process of water loss extraction from soil. This relaxes the requirement of data, including: i) meteorological data: air relative humidity, wind speed and solar radiation; ii) soil data, for instance water content at field capacity, soil texture and soil hydrologic conductivity. In evapotranspiration equation (4), the coefficients k_{E1} and k_{E2} are considered as the only parameters to be estimated, thus reducing the total number of estimated parameters. In addition, the percolation and runoff terms are represented as a lumped term called $R + G$, which is simple with no requirement of soil data. This is in contrast to the complexity of the curve number method for runoff. Due to these features, the application of the soil moisture dynamic models VHRAM, HDG0, HDG1, HDG3 and HDG4 to different soil types is facilitated. However, application of these models at specific sites requires calibration using daily measurements of soil moisture, precipitation, maximum air temperature, minimum air temperature and average air temperature.

Since the AIC value depends on the effect of both SSE and the number of parameters, a higher NS_0 value does not guarantee a lower AIC for a given model, whereas a high number of parameters may reduce the AIC, and the order of models is different for the AIC and NS_0 indices. For instance, the highest NS_0 value for the Calarcá station was obtained by the HDG4 model, but the lowest AIC was obtained by the HDG0 model. In addition, a high number of parameters does not guarantee a higher NS_0 for a given model (see Table 6). For instance, the HDG4 model has the largest number of parameters and exhibits the highest NS_0 value for Calarcá station (see Table 4), but not for Naranjal nor Balboa stations (see Tables 3 and 5). Recall that the number of parameters is: 14 (HDG4), 11 (HDG3), 9 (HDG1), 7 (VJRAM), 6 (HDG0), 6 (K7) and 6 (K8).

In general, models VJRAM and HDG0 achieved the lowest AIC values, considering the three weather stations. The higher performance of the VJRAM model for the Naranjal site indicates that the logarithmic structure of percolation term G is suitable for Naranjal station but not for Calarcá or Balboa stations. The higher performance of the HDG0 model for the Calarcá and Balboa stations in terms of AIC indicates its modelling capacity with a low number of parameters. The low performance of the K7 and K8 models confirms that the evapotranspiration term E has an important effect on the soil moisture model, and a proper expression must be used, whereas the Hargreaves model Eq (4) is suitable. Model HDG4 achieved a lower performance in terms of AIC, which is related to both its large number of parameters and its limited modelling capability in terms of NS_0.

Comparison of performance in different studies is not straightforward, because there are numerous factors influencing the performance of soil moisture modelling, including measurement uncertainty and model structure. Then, only model structure and modeling procedure is compared in what follows. The soil moisture modeling using models VJRAM, HDG0, HDG3 and HDG4 is simpler than that of [25]: the definition of the category of the soil moisture resistance curve, the fitting of the infiltration equation and the determination of the field capacity are not required. This leads to fewer measurements, and a simpler fitting procedure, whereas soil data are not required. Comparing soil moisture modelling in the present study with that of [22], a remarkable similarity is that the definition of the category of the soil moisture resistance curve, the preliminary fitting of infiltration equation and the determination of the field capacity are not required. In [22], the evapotranspiration term is a combination of exponential and logarithmic functions, and it requires measurement of wind speed, whereas the evapotranspiration term of models in the present study is based on the Hargreaves equation and requires measurement of T_{avg}, T_{max} and T_{min}. In [22], and also in our study with models HDG0, HDG4, HDG1 and HDG3, the percolation term depends on soil moisture and precipitation.

6. Conclusions

In this study, several empirical models are evaluated to estimate soil moisture for three locations in Colombia. The daily precipitation, and average, maximum and minimum air temperatures are the input variables. The first group of models are water balance types of models, where the evapotranspiration term is based on the Hargreaves model and is SM limited, whereas the runoff and percolation terms are functions of precipitation and soil moisture. The second group of models are simple compartment-based models. In addition, three models are proposed and formulated by combining the first model group with modifications in the precipitation, runoff, percolation and evapotranspiration terms, using functions recently proposed in current literature. The models are calibrated using field data from each location. The main contributions over closely related studies are:

i) a new model is proposed, based on a water balance model with terms from recent literature, and combinations of these terms are proposed; ii) the effect of model parameters on the fitting quality is assessed, and the parameters with higher effect are determined; iii) the proposed models and the empirical models reported in the recent literature are compared in terms of the combination of fitting accuracy and number of parameters, through the Akaike information criterion (AIC). The proposed modifications improved the simulation of soil moisture at the three locations.

The lowest AIC values correspond to the VJRAM, HDG0 and HDG0 models for the Naranjal, Calarcá and Balboa stations, respectively. In addition, the highest AIC values correspond to the K8, K7 and HDG3 models for the Naranjal, Calarcá and Balboa stations, respectively. Therefore, there is no single model that exhibits neither the highest nor the lowest capacity for representing the soil moisture in the three stations. However, the K7 and K8 models exhibited a lower modeling capacity in terms of AIC, compared to the HDG group and VJRAM, for the three stations. For the Naranjal station, the previous knowledge on percolation representation resulted in a higher capacity for modeling SM.

The Nash-Sutcliffe coefficient obtained was higher than 0.8 for the three stations. These NS_0 values can be considered as satisfactory, considering the complex soil effects supporting the variation of soil moisture and the lack of measurements of relative humidity, solar radiation and wind speed. The highest NS_0 values correspond to the VJRAM, HDG4 and HDG0 models, for the Naranjal, Calarcá and Balboa stations, respectively, whereas the lowest NS_0 values correspond to the K8, K7 and VJRAM models, for the Naranjal, Calarcá and Balboa stations, respectively. The HDG group of models exhibited a high NS_0 value for all cases. The use of a combination of polynomial terms of precipitation and soil moisture resulted in better NS_0 for the HDG3 model compared to HDG0, for the Naranjal and Calarcá stations.

Use of AI tools declaration

The authors declare that they have not used artificial intelligence (AI) tools in the creation of this article.

Acknowledgments

The work of Alejandro Rincón was supported by the Universidad Católica de Manizales. The work of Fredy E. Hoyos and John E. Candelo-Becerra was supported by the Universidad Nacional de Colombia, Sede Medellín. This work was also supported by the Universidad Nacional de Colombia, Sede Medellín, under the project HERMES: 55173.

The records of meteorological data for Calarcá and Balboa stations were collected from IDEAM database (http://www.ideam.gov.co/).

Conflict of interest

The authors declare there is no conflict of interest.

Appendix A

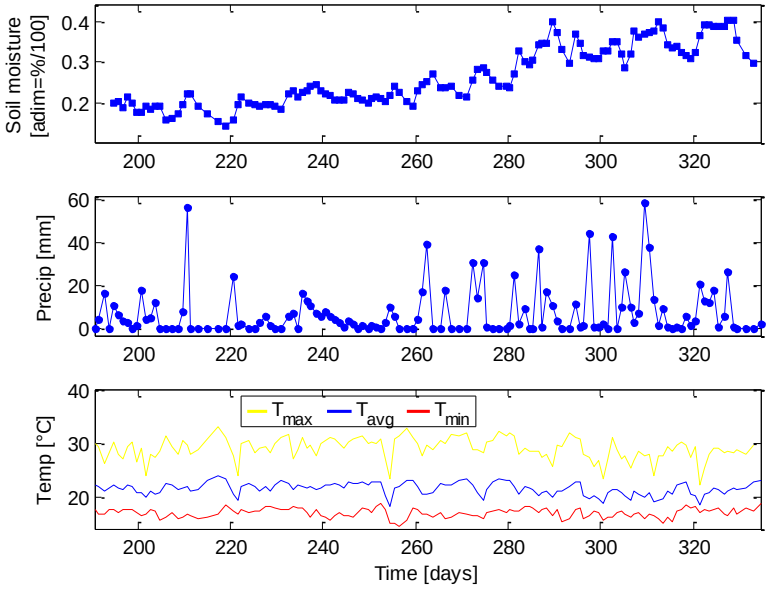

Figure A1. Time series of meteorological data at the Naranjal station.

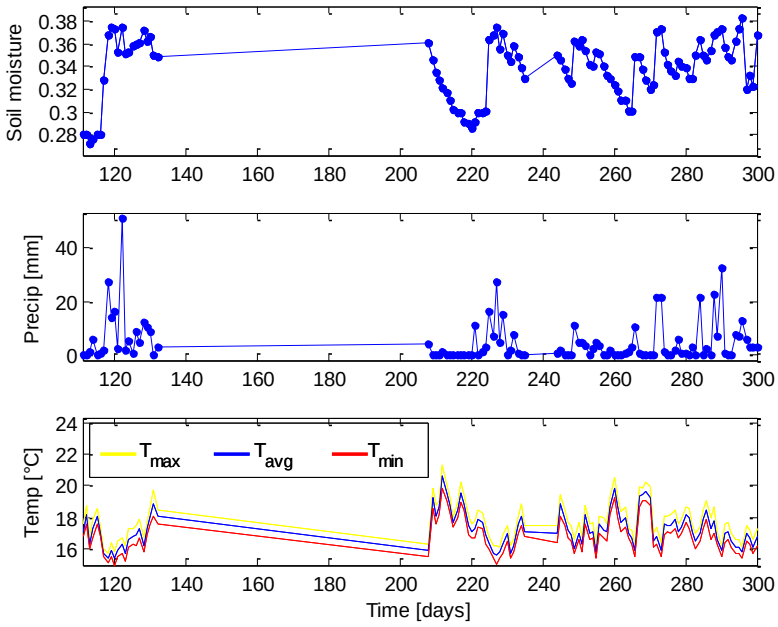

Figure A2. Time series of meteorological data at the Calarcá station.

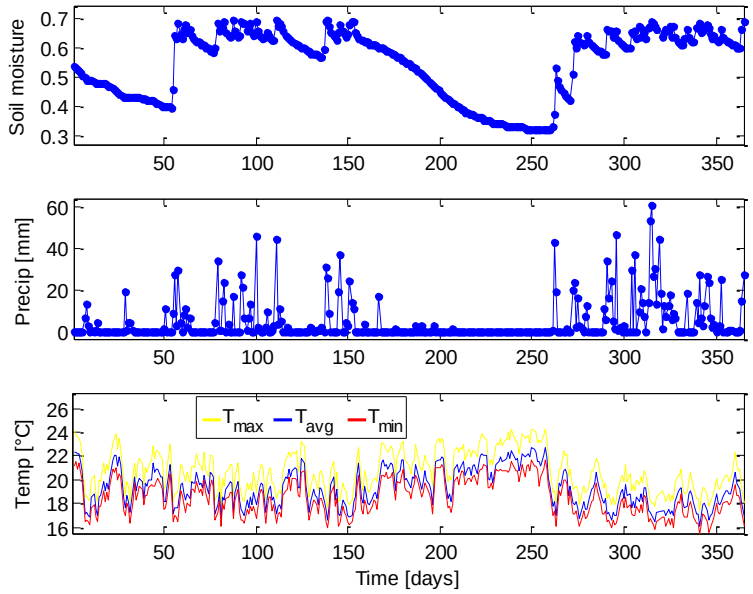

Figure A3. Time series of meteorological data at the Balboa station, period Ω_{B1}.

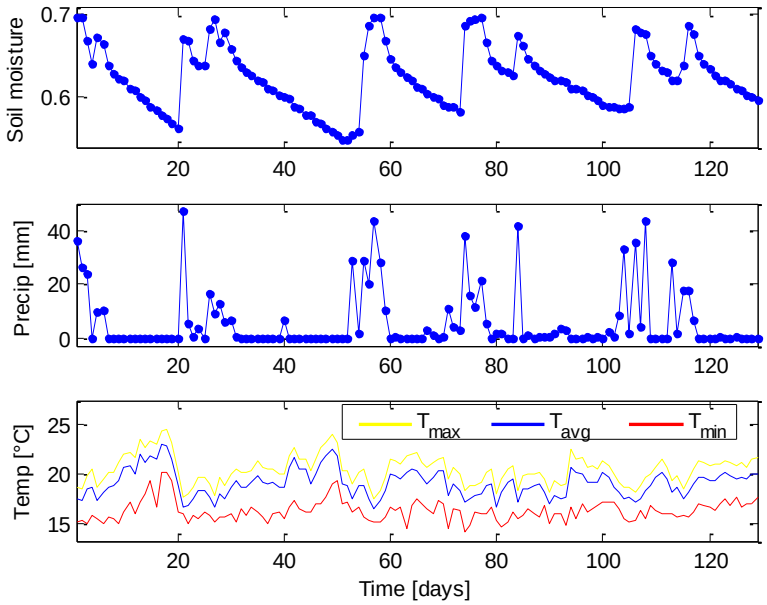

Figure A4. Time series of meteorological data at the Balboa station, period Ω_{B2}.

References

1. D. Jia, J. Wen, T. Zhang, J. Xi, Responses of soil moisture and thermal conductivity to precipitation in the mesa of the Loess Plateau, *Environm. Earth Sci.*, **75** (2016), 395. https://doi.org/10.1007/s12665-016-5350-x
2. M. Sadeghi, T. Hatch, G. Huang, U. Bandara, A. Ghorbani, E. C. Dogrul, Estimating soil water flux from single-depth soil moisture data, *J. Hydrol.*, **610** (2022), 127999.

https://doi.org/10.1016/j.jhydrol.2022.127999
3. M. Saeedi, A. Sharafati, L. Brocca, A. Tavakol, Estimating rainfall depth from satellite-based soil moisture data: A new algorithm by integrating SM2RAIN and the analytical net water flux models, *J. Hydrol.*, **610** (2022), 127868. https://doi.org/10.1016/j.jhydrol.2022.127868
4. S. A. Kannenberg, M. L. Barnes, D. R. Bowling, A. W. Driscoll, J. S. Guo, W. R. L. Anderegg, Quantifying the drivers of ecosystem fluxes and water potential across the soil-plant-atmosphere continuum in an arid woodland, *Agr. Forest Meteorol.*, **329** (2023), 109269. https://doi.org/10.1016/j.agrformet.2022.109269
5. K. A. Ishola, G. Mills, R. M. Fealy, Ó. N. Choncubhair, R. Fealy, Improving a land surface scheme for estimating sensible and latent heat fluxes above grasslands with contrasting soil moisture zones, *Agr. Forest Meteorol.*, **294** (2020), 108151. https://doi.org/10.1016/j.agrformet.2020.108151
6. J. Zhang, L. Duan, T. Liu, Z. Chen, Y. Wang, M. Li, et al., Experimental analysis of soil moisture response to rainfall in a typical grassland hillslope under different vegetation treatments, *Environ. Res.*, **213** (2022), 113608. https://doi.org/10.1016/j.envres.2022.113608
7. D. Rai, B. C. Kusre, P. K. Bora, L. Gajmer, A study on soil moisture model for agricultural water management under soil moisture stress conditions in Sikkim (India), *Sustain. Water Resour. Manag.*, **5** (2019), 1243–1257. https://doi.org/10.1007/s40899-018-0298-5
8. T. Yu, G. Jiapaer, G. Long, X. Li, J. Jing, Y. Liu, et al., Interannual and seasonal relationships between photosynthesis and summer soil moisture in the Ili River basin, Xinjiang, 2000–2018, *Sci. Total Environ.*, **856** (2023), 159191. https://doi.org/10.1016/j.scitotenv.2022.159191
9. T. Yu, G. Jiapaer, A. Bao, G. Zheng, J. Zhang, X. Li, et al., Disentangling the relative effects of soil moisture and vapor pressure deficit on photosynthesis in dryland Central Asia, *Ecolog. Indicat.*, **137** (2022), 108698. https://doi.org/10.1016/j.ecolind.2022.108698
10. R. Zhu, T. Hu, Q. Zhang, X. Zeng, S. Zhou, F. Wu, et al., A stomatal optimization model adopting a conservative strategy in response to soil moisture stress, *J. Hydrol.*, **617** (2023), 128931. https://doi.org/10.1016/j.jhydrol.2022.128931
11. M. Bassiouni, S. P. Good, C. J. Still, C. W. Higgins, Plant water uptake thresholds inferred from satellite soil moisture, *Geophys. Res. Letters*, **47** (2020), e2020GL087077. https://doi.org/10.1029/2020GL087077
12. S. Wang, R. Li, Y. Wu, W. Wang, Estimation of surface soil moisture by combining a structural equation model and an artificial neural network (SEM-ANN), *Sci. Total Environ.*, **876** (2023), 162558. https://doi.org/10.1016/j.scitotenv.2023.162558
13. K. Yang, H. Wang, L. Luo, S. Zhu, H. Huang, Z. Wei, et al., Effects of different soil moisture on the growth, quality, and root rot disease of organic Panax notoginseng cultivated under pine forests, *J. Environ. Manag.,* **329** (2023), 117069. https://doi.org/10.1016/j.jenvman.2022.117069
14. Z. Zhao, Y. Jiang, S. Yuan, M. Cui, D. Shi, F. Xue, et al., Inconsistent response times to precipitation and soil moisture in Picea crassifolia growth, *Dendrochronologia*, **77** (2023), 126032. https://doi.org/10.1016/j.dendro.2022.126032
15. J. Peng, C. Albergel, A. Balenzano, L. Brocca, O. Cartus, M. H. Cosh, et al., A roadmap for high-resolution satellite soil moisture applications— confronting product characteristics with user requirements, *Remote Sens. Environ.*, **252** (2021), 112162. https://doi.org/10.1016/j.rse.2020.112162
16. Z.-L. Li, P. Leng, C. Zhou, K.-S. Chen, F.-C. Zhou, G.-F. Shang, Soil moisture retrieval from remote sensing measurements: Current knowledge and directions for the future, *Earth-Sci. Rev.*,

218 (2021), 103673. https://doi.org/10.1016/j.earscirev.2021.103673
17. L. Zappa, S. Schlaffer, L. Brocca, M. Vreugdenhil, C. Nendel, W. Dorigo, How accurately can we retrieve irrigation timing and water amounts from (satellite) soil moisture?, *Int. J. Appl. Earth Observ. Geoinform.*, **113** (2022), 102979. https://doi.org/10.1016/j.jag.2022.102979
18. Z. Gu, T. Zhu, X. Jiao, J. Xu, Z. Qi, Neural network soil moisture model for irrigation scheduling, *Comput. Electron. Agr.*, **180** (2021), 105801. https://doi.org/10.1016/j.compag.2020.105801
19. R. Liao, S. Zhang, X. Zhang, M. Wang, H. Wu, L. Zhangzhong, Development of smart irrigation systems based on real-time soil moisture data in a greenhouse: Proof of concept, *Agr. Water Manag.*, **245** (2021), 106632. https://doi.org/10.1016/j.agwat.2020.106632
20. L. Liu, L. Gudmundsson, M. Hauser, D. Qin, S. Li, S. I. Seneviratne, Soil moisture dominates dryness stress on ecosystem production globally, *Nat. Commun.*, **11** (2020), 4892. https://doi.org/10.1038/s41467-020-18631-1
21. R. Moazenzadeh, B. Mohammadi, M. J. S. Safari, K.-W. Chau, Soil moisture estimation using novel bio-inspired soft computing approaches, *Eng. Appl. Comput. Fluid Mechan.*, **16** (2022), 826–840. https://doi.org/10.1080/19942060.2022.2037467
22. S. Verma, M. K. Nema, Development of an empirical model for sub-surface soil moisture estimation and variability assessment in a lesser Himalayan watershed, *Model. Earth Syst. Environ.*, **8** (2022), 3487–3505. https://doi.org/10.1007/s40808-021-01316-z
23. B. Panigrahi, S. N. Panda, Field test of a soil water balance simulation model, *Agr. Water Manag.*, **58** (2003), 223–240. https://doi.org/10.1016/S0378-3774(02)00082-3
24. J. Dari, P. Quintana-Seguí, R. Morbidelli, C. Saltalippi, A. Flammini, E. Giugliarelli, et al., Irrigation estimates from space: Implementation of different approaches to model the evapotranspiration contribution within a soil-moisture-based inversion algorithm, *Agr. Water Manag.*, **265** (2022), 107537. https://doi.org/10.1016/j.agwat.2022.107537
25. D. R. Legates, K. T. Junghenn, Evaluation of a simple, point-scale hydrologic model in simulating soil moisture using the Delaware environmental observing system, *Theor. Appl. Climatol.*, **132** (2018), 1–13. https://doi.org/10.1007/s00704-017-2041-9
26. J. L. Knopp, A minimal soil moisture model fit to environmental data from multiple pasture locations in Taranaki, New Zealand, *IFAC-PapersOnLine*, **53** (2020), 16703–16708. https://doi.org/10.1016/j.ifacol.2020.12.1109
27. J. Huang, H. M. van den Dool, K. P. Georgarakos, Analysis of model-calculated soil moisture over the United States (1931–1993) and applications to long-range temperature forecasts, *J. Climate*, **9** (1996), 1350–1362. https://doi.org/10.1175/1520-0442(1996)009<1350:AOMCSM>2.0.CO;2
28. J. Fidal, T. R. Kjeldsen, Accounting for soil moisture in rainfall-runoff modelling of urban areas, *J. Hydrol.*, **589** (2020), 125122. https://doi.org/10.1016/j.jhydrol.2020.125122
29. G. Pignotti, M. Crawford, E. Han, M. R. Williams, I. Chaubey, SMAP soil moisture data assimilation impacts on water quality and crop yield predictions in watershed modeling, *J. Hydrol.*, **617** (2023), 129122. https://doi.org/10.1016/j.jhydrol.2023.129122
30. J.-F. Mahfouf, B. Jacquemin, A study of rainfall interception using a 1And surface parameterization for mesoscale meteorological models, *J. Meteorol. Climatol.*, **28** (1989), 1282–1302. https://doi.org/10.1175/1520-0450(1989)028<1282:ASORIU>2.0.CO;2
31. D. E. Carlyle-Moses, J. H. C. Gash, Rainfall Interception Loss by Forest Canopies, in *Forest Hydrology and Biogeochemistry: Synthesis of Past Research and Future Directions* (eds. D. F. Levia, D. Carlyle-Moses, T. Tanaka), (2011), 407–423. https://doi.org/10.1007/978-94-007-1363-

5_20
32. A. Jaramillo-Robledo, B. Cháves-Córdoba, Aspectos hidrológicos en un bosque y en plantaciones de café (Coffea arabica L.) al sol y bajo sombra, *Cenicafé,* **50** (1999), 97–105.
33. F. Pan, C. D. Peters-Lidard, M. J. Sale, An analytical method for predicting surface soil moisture from rainfall observations, *Water Resour. Res.*, **39** (2003), 1314. https://doi.org/10.1029/2003wr002142
34. M. Ruichen, S. Jinxi, T. Bin, X. Wenjin, K. Feihe, S. Haotian, et al., Vegetation variation regulates soil moisture sensitivity to climate change on the Loess Plateau, *J. Hydrol.*, **617** (2023), 128763. https://doi.org/10.1016/j.jhydrol.2022.128763
35. L. Li, D. Wu, T. Wang, Y. Wang, Effect of topography on spatiotemporal patterns of soil moisture in a mountainous region of Northwest China, *Geoderma Regional*, **28** (2022), e00456. https://doi.org/10.1016/j.geodrs.2021.e00456
36. V. Y. Chandrappa, B. Ray, N. Ashwatha, P. Shrestha, Spatiotemporal modeling to predict soil moisture for sustainable smart irrigation, *Internet Things*, **21** (2023), 100671. https://doi.org/10.1016/j.iot.2022.100671
37. K. Djaman, A. B. Balde, A. Sow, B. Muller, S. Irmak, M. K. N'Diaye, et al., Evaluation of sixteen reference evapotranspiration methods under sahelian conditions in the Senegal River Valley, *J. Hydrol. Regional Studies*, **3** (2015), 139–159. https://doi.org/10.1016/j.ejrh.2015.02.002
38. D. Dlouhá, V. Dubovský, L. Pospíšil, Optimal calibration of evaporation models against Penman–Monteith equation, *Water*, **13** (2021), 1484. https://doi.org/10.3390/w13111484
39. R. Hadria, T. Benabdelouhab, H. Lionboui, A. Salhi, Comparative assessment of different reference evapotranspiration models towards a fit calibration for arid and semi-arid areas, *J. Arid Environ.*, **184** (2021), 104318. https://doi.org/10.1016/j.jaridenv.2020.104318
40. V. Sheikh, S. Visser, L. Stroosnijder, A simple model to predict soil moisture: Bridging Event and Continuous Hydrological (BEACH) modelling, *Environ. Model.Software*, **24** (2009), 542–556. https://doi.org/10.1016/j.envsoft.2008.10.005
41. P. Bogawski, E. Bednorz, Comparison and validation of selected evapotranspiration models for conditions in Poland (Central Europe), *Water Resour. Manag.*, **28** (2014), 5021–5038. https://doi.org/10.1007/s11269-014-0787-8
42. R. G. Allen, L. S. Pereira, D. Raes, M. Smith, Crop evapotranspiration: Guidelines for computing crop water requirements, *FAO Food Agr. Organiz. United Nations,* FAO Irrigation and drainage, (1998), 56.
43. S. V. Franco, A. J. Robledo, Redistribution of rainfall in different vegetation covers of the central coffee zone of Colombia, *Cenicafé,* **60** (2009), 148–160.
44. V. H. Ramírez-Builes, Á. Jaramillo-Robledo, J. Arcila-Pulgarín, E. C. Montoya-Restrepo, Estimation of Soil Moisture in Coffee Plantations with Free Sun Exposure, Cenicafé, **61** (2010), 251–259.
45. K. I. Islam, A. Khan, T. Islam, Correlation between atmospheric temperature and soil temperature: A case study for Dhaka, Bangladesh*, Atmosph. Climate Sci.*, **5** (2015), 200–208. https://doi.org/10.4236/acs.2015.53014
46. W. C. Forsythe, E. J. Rykiel, R. S. Stahl, H.-I. Wu, R. M. Schoolfield, A model comparison for daylength as a function of latitude and day of year, *Ecolog. Model.*, **80** (1995), 87–95. https://doi.org/10.1016/0304-3800(94)00034-F
47. S. A. Banimahd, D. Khalili, S. Zand-Parsa, A. A. Kamgar-Haghighi, Groundwater potential

recharge estimation in bare soil using three soil moisture accounting models: Field evaluation for a semi-arid foothill region, *Arabian J. Geosci.*, **10** (2017), 223. https://doi.org/10.1007/s12517-017-3018-9

48. E.-M. Hong, W.-H. Nam, J.-Y. Choi, Y. A. Pachepsky, Projected irrigation requirements for upland crops using soil moisture model under climate change in South Korea, *Agr. Water Manag.*, **165** (2016), 163–180. https://doi.org/10.1016/j.agwat.2015.12.003
49. L. N. Bermúdez-Florez, J. R. Cartagena-Valenzuela, V. H. Ramírez-Builes, Soil humidity and evapotranspiration under three coffee (Coffea arabica L.) planting densities at Naranjal experimental station (Chinchiná, Caldas, Colombia), *Acta Agronóm.*, **67** (2018), 402–413. https://doi.org/10.15446/acag.v67n3.67377
50. F. J. H. Guzmán, Evaluation of agroclimatic methods for the timely estimation of soil surface moisture conditions in agricultural areas of Colombia, Master Thesis, Universidad Nacional de Colombia (2021).
51. M. Littleboy, D. M. Silburn, D. M. Freebairn, D. R. Woodruff, G. L. Hammer, J. K. Leslie, Impact of soil erosion on production in cropping systems I, Development and validation of a simulation model, *Soil Res.*, **30** (1992), 757. https://doi.org/10.1071/sr9920757
52. D. Liu, C. Liu, Y. Tang, C. Gong, A GA-BP neural network regression model for predicting soil moisture in slope ecological protection, *Sustain. Sci. Pract. Pol.*, **14** (2022), 1386. https://doi.org/10.3390/su14031386
53. J. Elliott, J. Price, Comparison of soil hydraulic properties estimated from steady-state experiments and transient field observations through simulating soil moisture in regenerated Sphagnum moss, *J. Hydrol.*, **582** (2020), 124489. https://doi.org/10.1016/j.jhydrol.2019.124489
54. M. Bassiouni, S. Manzoni, G. Vico, Optimal plant water use strategies explain soil moisture variability, *Adv. Water Resour.*, **173** (2023), 104405. https://doi.org/10.1016/j.advwatres.2023.104405
55. V. H. G. Díaz, M. J. Willis, Ethanol production using Zymomonas mobilis: Development of a kinetic model describing glucose and xylose co-fermentation, *Biomass Bioenergy*, **123** (2019), 41–50. https://doi.org/10.1016/j.biombioe.2019.02.004
56. S. Portet, A primer on model selection using the Akaike Information Criterion, *Infect. Disease Modell.*, **5** (2020), 111–128. https://doi.org/10.1016/j.idm.2019.12.010
57. K. Dutta, Substrate inhibition growth kinetics for cutinase producing Pseudomonas cepacia using tomato-peel extracted cutin, *Chem. Biochem. Eng. Quarterly*, **29** (2015), 437–445. https://doi.org/10.15255/cabeq.2014.2022

AIMS Press